

This is an Open Access document downloaded from ORCA, Cardiff University's institutional repository: <https://orca.cardiff.ac.uk/id/eprint/143977/>

This is the author's version of a work that was submitted to / accepted for publication.

Citation for final published version:

Heise, Denise, Derrac Soria, Alicia, Hansen, Selina, Dambietz, Christine, Akbarzadeh, Mohammad, Berg, Anna F., Waetzig, Georg H., Jones, Simon A. , Dvorsky, Radovan, Ahmadian, Mohammad R., Scheller, Jürgen and Moll, Jens M. 2021. Selective inhibition of IL-6 trans-signaling by a miniaturized, optimized chimeric soluble gp130 inhibits TH17 cell expansion. *Science Signaling* 14 (696) , eabc3480. 10.1126/scisignal.abc3480

Publishers page: <http://dx.doi.org/10.1126/scisignal.abc3480>

Please note:

Changes made as a result of publishing processes such as copy-editing, formatting and page numbers may not be reflected in this version. For the definitive version of this publication, please refer to the published source. You are advised to consult the publisher's version if you wish to cite this paper.

This version is being made available in accordance with publisher policies. See <http://orca.cf.ac.uk/policies.html> for usage policies. Copyright and moral rights for publications made available in ORCA are retained by the copyright holders.





**One-sentence summary:** Smaller, more selective molecular traps of IL-6 trans-signaling complexes may treat autoimmunity.

**Editor's summary:**

**Precision blockade of inflammatory IL-6**

The cytokine IL-6 performs critical functions in various tissue types but is implicated in autoimmune disease. Therefore, precisely targeting the pathway by which IL-6 induces inflammatory immune cell activation could leave other signaling pathways and functions of IL-6 intact. Currently, such targeted molecules lack sufficient selectivity. Heise *et al.* developed a chimeric molecule that bound to and “trapped” a critical IL-6 trans-signaling protein complex and that was smaller, had greater selectivity for the IL-6 complex over a similar IL-11 complex, and more effectively inhibited the IL-6–induced inflammatory activation of cultured T cells. These findings may lead to improved therapeutics for patients with autoimmune disease.

**Selective inhibition of IL-6 trans-signaling by a miniaturized, optimized chimeric soluble gp130 inhibits T<sub>H</sub>17 cell expansion<sup>†</sup>**

Denise Heise<sup>1§</sup>, Alicia Derrac Soria<sup>2§</sup>, Selina Hansen<sup>1§</sup>, Christine Dambietz<sup>1</sup>, Mohammad Akbarzadeh<sup>1#</sup>, Anna F. Berg<sup>1</sup>, Georg H. Waetzig<sup>3,4</sup>, Simon Jones<sup>2</sup>, Radovan Dvorsky<sup>1</sup>, Mohammad R. Ahmadian<sup>1</sup>, Jürgen Scheller<sup>1\*</sup>, Jens M. Moll<sup>1\*</sup>

<sup>1</sup>Institute of Biochemistry and Molecular Biology II, Medical Faculty, Heinrich-Heine-University, 40225 Düsseldorf, Germany.

<sup>2</sup> Division of Infection and Immunity, School of Medicine, Systems Immunity University Research Institute, College of Biomedical and Life Sciences, Cardiff University, CF14 4XN Cardiff, United Kingdom.

<sup>3</sup>Institute of Clinical Molecular Biology, Kiel University and University Medical Center Schleswig-Holstein, 24105 Kiel, Germany.

<sup>4</sup>CONARIS Research Institute AG, 24118 Kiel, Germany.

<sup>#</sup>Current address: Max-Planck-Institut für Molekulare Physiologie, Chemische Biologie, 44227, Dortmund, Germany.

<sup>§</sup>These authors contributed equally.

<sup>\*</sup>Corresponding author. Email: jscheller@uni-duesseldorf.de (J.S.), jens.moll@uni-duesseldorf.de (J.M.M.)

**Abstract:**

The cytokine interleukin-6 (IL-6) signals through three mechanisms called classic signaling, trans-signaling, and trans-presentation. IL-6 trans-signaling is distinctly mediated through a soluble form of its transmembrane receptor IL-6R (sIL-6R) and the coreceptor gp130 and is implicated in multiple autoimmune diseases. Although a soluble form of gp130 (sgp130) inhibits

only IL-6 trans-signaling, it also blocks an analogous trans-signaling mechanism of IL-11 and its soluble receptor sIL-11R. Here, we report miniaturized chimeric soluble gp130 variants that efficiently trap IL-6:sIL-6R but not IL-11:sIL-11R complexes. We designed a novel IL-6 trans-signaling trap by fusing a miniaturized sgp130 variant to an IL-6:sIL-6R complex-binding nanobody and the Fc portion of immunoglobulin G (IgG). This trap, called cs-130Fc exhibited improved inhibition of as well as increased selectivity for IL-6 trans-signaling compared to the conventional fusion protein sgp130Fc. We introduced affinity-enhancing mutations in cs-130Fc and sgp130Fc that further improved selectivity towards IL-6 trans-signaling. Moreover, cs-130Fc efficiently inhibited the expansion of T helper 17 (T<sub>H</sub>17) cells in cultures of mouse CD4<sup>+</sup> T cells treated with IL-6:sIL-6R. Thus, these variants may provide or lead to the development of more precisely targeted therapeutics for inflammatory disorders associated with IL-6 trans-signaling.

## Introduction

Interleukin-6 (IL-6) is a cytokine involved in a plethora of processes that include inflammation, acute phase response, infection, neurodegenerative processes, autoimmunity, and trauma (1). IL-6 exerts its effects by different mechanisms depending on the target cells. Classic IL-6 signaling, which mainly controls acute inflammatory responses, such as the acute phase reaction, is induced by binding of IL-6 to its membrane-bound receptor IL-6R on target cells (2). This event is followed by recruitment of the ubiquitously expressed signal-transducing co-receptor gp130 and initiation of downstream signaling cascades leading to activation of the Janus kinase/signal transducer and activator of transcription (JAK/STAT), protein kinase B (PKB or AKT) and mitogen-activated protein kinase (MAPK) pathways. In contrast, “IL-6 trans-signaling” occurs through the formation of a complex between IL-6 and soluble forms of the IL-6R (sIL-6R) (2); these complexes can activate downstream signaling cascades in all cells expressing gp130. Increased or dysregulated IL-6 trans-signaling is observed in many chronic inflammatory diseases, including rheumatoid arthritis (3, 4), multiple sclerosis (5), inflammatory bowel disease (6-8), and cancer (9-11). Some dendritic cells do not express gp130 but IL-6R; these cells are able to induce a third mechanism of IL-6 signal transduction called “IL-6 trans-presentation” (12, 13). For IL-6 trans-presentation, IL-6 binds to membrane-bound IL-6R on a transmitter cell, and the resulting complex engages gp130 on a different, so-called receiver cell and activate signal transduction through gp130 dimerization.

Targeting IL-6 signaling is of therapeutic interest for many diseases. However, global IL-6 blockade, such as with IL-6 antibodies, is associated with many side effects (including an increased risk of bacterial and viral infections) (14, 15) due to the multitude of functions of this cytokine. Hence, to efficiently target distinct disease-specific IL-6 functions, it is important to both understand the mode of IL-6 signaling in the disease process and have the ability to selectively target that mode. IL-6 has three binding sites for its receptors: site I recognizes IL-6R, while sites II and III establish the contact to gp130. IL-6 or IL-6R antibodies usually target the site I interface formed between IL-6 and the IL-6R and affect both classic and trans-signaling.

The fusion protein sgp130Fc targets sites II and III and does not, in principle, affect IL-6 classic signaling, unless extremely high concentrations are used that enable quantitative complexing of IL-6 with sIL-6R and, thus, can reduce free IL-6 levels (16).

Therefore, in contrast to neutralizing antibodies, the control of bacterial and viral infections is not expected to be affected by sgp130Fc, which is supported by mouse experiments (17). A phase II study with soluble gp130 (Olamkicept) (EudraCT, Number 2016-000205-36) demonstrated the safety and efficacy of sgp130 in the treatment of Crohn's disease and ulcerative colitis. However, sgp130(Fc) inhibits IL-11 trans-signaling with similar potency as IL-6 trans-signaling (18). The physiological role of IL-11 trans-signaling is currently not understood. There is clear evidence for the presence of IL-11/sIL-11R complexes in human serum and that these complexes are able to activate cells through IL-11 trans-signaling (18). In addition, leukemia inhibitory factor (LIF) and oncostatin M (OSM) signaling are also affected by high concentrations of sgp130Fc (19, 20). Moreover, sgp130Fc is a very large molecule; it is a protein dimer of approximately 186 kDa plus 20 glycosylation chains, leading to an apparent molecular weight of about 240 kDa. Efforts have been made to reduce the size of the molecule using also naturally occurring sgp130 monomers (120 kDa) or the short sgp130-RAPS variant consisting of only the ligand-binding domains D1-D3 of gp130 (50 kDa), but the inhibitory capacities and binding affinities of these proteins were 10–1,000 fold lower than those of sgp130Fc dimers (20–22). Here, we present a novel class of chimeric soluble gp130-based IL-6 trans-signaling inhibitors (cs-130Fc). cs-130Fc variants are composed of cytokine binding domains of sgp130 fused to a nanobody specifically binding to IL-6:sIL-6R complexes (VHH6) (23). The most efficient cs-130Fc fusion proteins had improved inhibitory activity for IL-6 trans-signaling over sgp130Fc. We further demonstrated a clear selectivity for IL-6 over IL-11 trans-signaling of cs-130Fc variants, in contrast to sgp130Fc.

## Results

### *Design and production of miniaturized sgp130 variants*

Albeit that sgp130Fc is a very potent IL-6 trans-signaling inhibitor (20), it is a rather large dimer of approximately 240 kDa (186 kDa protein plus glycosylation), even compared to, *e.g.*, therapeutic IgG antibodies (150 kDa). For antibodies and their fragments, a clear correlation between biodistribution and molecular weight has been demonstrated (24). Several smaller variants of sgp130 including monomeric variants lacking the Fc part or the natural short sgp130-RAPS isoform were characterized previously (20, 22, 25). These studies demonstrated that, for unknown reasons, the activity of sgp130-based trans-signaling inhibitors inversely correlates with their molecular weight. sgp130Fc inhibits IL-6 trans-signaling with an  $IC_{50}$  of 77 pM (20), the  $IC_{50}$  of monomeric sgp130 is above 700 pM (20) and the  $IC_{50}$  for sgp130-RAPS is well over 70 nM (22). We aimed to obtain novel fusion proteins with biological activities comparable to sgp130Fc but much lower molecular weights. To this end, we designed miniaturized sgp130 variants composed of combinations of the cytokine binding domains D1 and D2-D3,

respectively. To improve their inhibitory potential, we fused these sgp130 domains with a previously described single domain antibody (sdAb, VHH, nanobody) recognizing the interface formed by IL-6 in complex with the IL-6R (VHH6) (23). The sdAb recognizes only the complex of IL-6 and sIL-6R, but not the individual components (23). The sdAb binds the complex of IL-6 and the sIL-6R with nanomolar affinity and, based on the dissociation rate constant, stabilizes the complex (23). By combining the sgp130 ligand-binding domains and the sdAb, we expected to obtain avidity effects restoring the biological activity lost through miniaturization of sgp130. Fusion proteins were designed as follows: The first three domains of sgp130 also included in the sgp130-RAPS variant (22) were connected to a flexible linker, followed by the sdAb VHH6 and a tobacco etch virus (TEV) protease recognition site. An Fc domain was used to generate dimeric inhibitors that, similar to the natural membrane-bound receptor gp130, are able to contact complexes of IL-6:sIL-6R via site II and site III, thereby completely enclosing them. We were aiming for enabling the inhibitors to contact site II and III residues simultaneously through dimeric design and hence obtain more efficient inhibitors through avidity effects. The resulting fusion protein labeled cs-130Fc has a theoretical molecular weight of 157 kDa compared to 186 kDa for sgp130Fc (Fig. 1A). After TEV cleavage, the resulting cs-130 was expected to have a molecular weight of about 52 kDa. A variety of fusion proteins were generated to investigate the effects of the domains D1-D3 of sgp130 and the sdAb components in terms of inhibitory function (Fig. 1B). To evaluate effects of the sdAb component, c<sub>GFP</sub>S-130Fc was generated, which contains a sdAb directed against instead of the IL-6/sIL-6R complex. In additional variants, mutations were introduced in the D1 and D2 domains of sgp130 to reduce or increase binding affinity to the IL-6:sIL-6R complex termed cs-130<sup>Y190K/F191E</sup>Fc (26) and cs-130<sup>T102Y/Q113F/N114L</sup>Fc, respectively (27) (Fig. 1B).

cs-130Fc variants containing domains D1-D3 of sgp130Fc were readily expressed and secreted by CHO-K1 cells (Fig. 2A). sgp130Fc and cs-130Fc variants were detected at slightly higher molecular weights (120 and 100 kDa, respectively) than the theoretical molecular weight (93 and 78 kDa, respectively), which is likely due to glycosylation. However, miniaturized variants containing only the D1 or the D2-D3 domains were poorly expressed and secreted. Consequently, only variants containing domains D1-D3 of sgp130 were considered for further characterization. cs-130Fc variants were expressed by stably transfected CHO-K1 cells and affinity-purified from cell culture supernatants. Following affinity purification, proteins were pure, as demonstrated by SDS-PAGE analysis and subsequent Coomassie staining (Fig. 2B). Purified cs-130Fc was processed with TEV protease to remove the Fc segment. Proteolytic processing yielded three molecular species with molecular weights of approximately 100, 70 and 25 kDa consistent with the presence of unprocessed protein (78 kDa), cs-130 (52 kDa) and the Fc fragment (26 kDa), respectively (Fig. 2C). The resulting fragments were separated by size exclusion chromatography (SEC). Further analysis using non-reducing SDS-PAGE (Fig. 2D) confirmed the absence of the Fc sequence from the 70 kDa cs-130 fragment. In the absence of reducing agent, sgp130Fc and cs-130Fc fusion proteins migrated corresponding to dimeric proteins with molecular weights above 170 kDa. In the presence of reducing agent, molecular

weights of both proteins dropped to approximately 120 and 100 kDa, corresponding to monomeric sgp130Fc and cs-130Fc. Following Fc removal, cs-130 displayed a reduction of molecular weight to 70 kDa independent of the presence of reducing agent. This further indicated the successful removal of the Fc fragment. The quality and molecular mass of the purified proteins was subsequently assessed in solution via analytical size exclusion chromatography coupled to multi angle light scattering (SEC-MALS) (Fig. 2E). All samples displayed minor peaks corresponding to aggregated protein (<10%), while the main peaks contained approximately 90% of the sample. For all proteins, molecular masses close to the theoretical masses were determined (summarized in Table 1). Minor differences between estimated molecular weight and theoretical molecular weight of approximately 20% are likely due to glycosylation. For cs-130, an additional conjugate analysis using dn/dc values for proteins and sugars was performed to determine the composition of the protein. A total mass of 75 kDa was determined, composed of 58 kDa protein and 17 kDa sugar components (Fig. 2F). The protein mass determined was in accordance with the theoretical molecular weight of 52 kDa.

### ***cs-130Fc and cs-130 fusion proteins display improved IL-6 trans-signaling inhibition in comparison to sgp130***

The kinetics of cs-130Fc binding to the IL-6/sIL-6R fusion protein hyper-IL-6 binding were characterized using surface plasmon resonance. Hyper-IL-6 was immobilized on a CM5 chip, and inhibitory proteins were injected at increasing concentrations. Binding of the inhibitory proteins resulted in the sensorgrams displayed in Fig. 3A. Striking differences in the dissociation rate constants were observed (Fig. 3 A and B). For sgp130Fc a  $k_{\text{off}}$  of  $7.2 \times 10^{-5} \text{ s}^{-1}$  was determined, while cs-130Fc showed a dissociation rate constant of  $3.6 \times 10^{-8} \text{ s}^{-1}$  which is significantly lower than sgp130Fc. This indicates that incorporation of VHH6 strongly increased the stability of the hyper-IL-6/cs-130Fc complexes, which is in good agreement with the previously described stabilization effect of VHH6 on IL-6/sIL-6R complexes (23).

Next, we examined the capacity of cs-130 variants to interfere with IL-6 trans-signaling in a model system of Ba/F3 cells stably transduced with gp130 (Ba/F3-gp130). These cells respond to IL-6 trans-signaling with STAT3 activation and proliferation. To test dimeric and monomeric cs-130 variants, we stimulated Ba/F3-gp130 cells with 50 ng/ml IL-6 and 100 ng/ml sIL-6R or with 10 ng/ml hyper-IL-6-Fc in the presence of increasing concentrations of the inhibitory proteins (Fig. 3C). sgp130Fc potently inhibited proliferation with an  $\text{IC}_{50}$  of 0.87 nM (Table 2), while cs-130Fc displayed improved inhibitory activity with an  $\text{IC}_{50}$  value of 0.27 nM. The negative control proteins  $\text{c}_{\text{GFPS}}$ -130Fc (comprising a GFP-specific nanobody instead of VHH6) and cs-130<sup>Y190K/F191E</sup>Fc (comprising two affinity-reducing point mutations in the CBM of sgp130Fc) (26) had markedly reduced biological activities with  $\text{IC}_{50}$  values of 6.54 nM and 7.55 nM, respectively. Also monomeric cs-130 potently inhibited IL-6:sIL-6R induced proliferation with an  $\text{IC}_{50}$  of 1.46 nM comparable to sgp130Fc. All  $\text{IC}_{50}$  values are summarized in Table 2. For monomeric sgp130 and dimeric sgp130Fc, an approximately 10-fold difference in biological

activity has been described previously (20). The apparent differences between IC<sub>50</sub> values of dimeric cs-130Fc and its monomeric counterpart cs-130 are comparable to the differences of sgp130 dimers and monomers and may be explained by avidity effects.

Subsequently, we investigated whether the above findings could be confirmed in orthogonal assays. We analyzed STAT3 and ERK phosphorylation as the important second messenger of IL-6 trans-signaling. STAT3 and ERK phosphorylation was analyzed in Ba/F3-gp130 cells. Cells were stimulated with 50 ng/ml IL-6 and 100 ng/ml sIL-6R in the presence of increasing concentration of inhibitory proteins. Concentration-dependent inhibition of STAT3 phosphorylation was observed for all inhibitory proteins (Fig. 3D). sgp130Fc completely suppressed STAT3 phosphorylation at a concentration of 10 nM. At 1 nM sgp130Fc, STAT3 phosphorylation was strongly reduced, while only a minor reduction was observed at 0.1 nM. Similarly to the effects observed in proliferation assays, cs-130Fc displayed potent inhibitory potential on STAT3 phosphorylation comparable to sgp130Fc. Monomeric cs-130 inhibited STAT3 phosphorylation at concentrations of 10 and 1 nM, while at 0.1 nM in contrast to sgp130Fc and its dimeric counterpart no inhibition was observed. The affinity-compromised variants c<sub>GFP</sub>S-130Fc and cs-130<sup>Y190K/F191E</sup>Fc displayed inhibitory activity, however, higher concentrations were required of these inhibitors to obtain full inhibition (Fig. 3D). In addition, a trend indicating a possible reduction of ERK phosphorylation was observed (fig. S1).

In contrast to other IL-6 signaling inhibitors like monoclonal antibodies, sgp130Fc is specific for trans-signaling and only affects IL-6 classic signaling at very high doses when sIL-6R is in excess over IL-6 (16). To exclude an effect on classic signaling, we tested cs-130Fc variants on Ba/F3-gp130-IL-6R cells (additionally stably transduced with IL-6R), which were stimulated with IL-6. Proliferation assays with Ba/F3-gp130-IL-6R cells revealed that sgp130Fc and cs-130Fc variants did not inhibit IL-6 classic-signaling at the concentrations tested (and in the absence of sIL-6R), while tocilizumab (28, 29), a monoclonal antibody directed against site 1 of the IL-6R, did inhibit signaling as expected (fig. S2).

### ***cs-130Fc variants do not inhibit IL-11 trans-signaling***

Next, we determined affinity constants for the interaction of the different inhibitory proteins with hyper-IL-11-Fc, a fusion protein of IL-11 and sIL-11R analogous to hyper-IL-6, of which two fusion proteins are dimerized by an Fc part. Hyper-IL-11-Fc was immobilized on a CM-5 chip, and binding of injected inhibitors was analyzed via surface plasmon resonance (Fig. 4A). Observed kinetic parameters are summarized in Table 3. It was found that sgp130Fc bound to hyper-IL-11-Fc with approximately 28-fold higher affinity ( $K_d = 0.3$  nM) than cs-130Fc ( $K_d = 8.6$  nM). sgp130 efficiently block IL-6 trans-signaling but are not restricted to IL-6. sgp130Fc also inhibits IL-11 trans-signaling (13) and, albeit to a much lesser extent, also affects LIF and OSM signaling (19). We chose an IL-11 trans-signaling model to investigate whether the incorporation of the IL-6/sIL-6R single domain antibody VHH6 into the cs-130Fc variants resulted in improved IL-6 trans-signaling specificity over sgp130Fc. First, we performed

proliferation assays using Ba/F3-gp130 cells stimulated with IL-11 and sIL-11R (Fig. 4B). We found that sgp130Fc was 32 times more potent in blocking IL-11 trans-signaling than cs-130Fc with  $IC_{50}$  values of 0.2 and 7.1 nM, respectively (Table 2). Moreover, cs-130Fc and c<sub>GFP5</sub>-130Fc displayed very similar  $IC_{50}$  values of 7.1 and 16.7 nM for IL-11 trans-signaling, indicating that VHH6 had no effects on the formation or stabilization of the IL-11/sIL-11R complex. Under the conditions used, monomeric cs-130 had no effect on IL-11 trans-signaling, similarly to mutationally inactivated cs-130Fc<sup>Y190K/F191E</sup>Fc. These findings were confirmed by analysis of the phosphorylation status of STAT3 and ERK after stimulation of Ba/F3-gp130 cells with 400 ng/ml IL-11 and 800 ng/ml sIL-11R (Fig. 4C, fig. S3). Analogous to the effects observed in proliferation assays, sgp130Fc was most potent in blocking IL-11 trans-signaling induced STAT3 and ERK phosphorylation. STAT3 phosphorylation was completely inhibited by 1 and 10 nM sgp130Fc, whereas cs-130Fc only induced a reduction of STAT3 phosphorylation at 10 nM concentrations, similar to the c<sub>GFP5</sub>-130Fc control. cs-130 and cs-130<sup>Y190K/F191E</sup>Fc had no significant effect on IL-11 trans-signaling-induced STAT3 phosphorylation.

### ***Affinity-enhancing mutations improve inhibitory capacity and selectivity of sgp130Fc and cs-130Fc variants***

sgp130Fc is a well-characterized IL-6 trans-signaling inhibitor. IL-6 interacts with the IL-6R at its binding site I and with gp130 at sites II and III. The identity of residues at the interfaces of these contact sites was found by crystallographic studies and extensive mutagenesis (30, 31). Previously, we described mutations in sgp130 associated with improved affinity of sgp130 towards IL-6 (27). We were interested, therefore, whether IL-6 affinity-boosting mutations of sgp130 impact the effects of sgp130 on IL-11 trans-signaling. Consequently, we compared the inhibitory profiles of sgp130Fc and the sgp130Fc mutein sgp130<sup>T102Y/Q113F/N114L</sup>Fc (27), which incorporates three point mutations at site III (Fig. 5A), with regard to their ability to inhibit trans-signaling of IL-6 and IL-11. Both proteins potently inhibited proliferation of the standard trans-signaling model cell line Ba/F3 stably transduced with gp130 (Ba/F3-gp130), when the cells were stimulated with 50 ng/ml IL-6 and 100 ng/ml sIL-6R (Fig. 5B). A profound difference of the inhibitory profile of both proteins was apparent for Ba/F3-gp130 cells stimulated with 10 ng/ml IL-11 and 100 ng/ml sIL-11R (Fig. 5C). Whereas sgp130Fc efficiently inhibited IL-11 trans-signaling induced proliferation, an approximately 25-fold higher dose of the sgp130<sup>T102Y/Q113F/N114L</sup>Fc mutein was required to obtain a similar level of inhibition. In conclusion, our data showed that improving the affinity of sgp130 for IL-6 trans-signaling almost completely prevented the inhibition of IL-11 trans-signaling. Next, the mutations T102Y, Q113F and N114L at site III of sgp130 were introduced into cs-130Fc to further improve its affinity towards IL-6. The resulting cs-130<sup>T102Y/Q113F/N114L</sup>Fc was expressed and purified by affinity chromatography (fig. S4). Monomeric cs-130<sup>T102Y/Q113F/N114L</sup> was then generated by TEV protease cleavage of the Fc fragment and isolated by SEC (fig. S4). Both the dimeric cs-130<sup>T102Y/Q113F/N114L</sup>Fc and the monomeric cs-130<sup>T102Y/Q113F/N114L</sup> efficiently inhibited IL-6 trans-

signaling-induced proliferation of Ba/F3-gp130 cells with IC<sub>50</sub> values of 0.36 and 0.48 nM, respectively (Fig. 6A and Table 2). In comparison, for sgp130Fc an IC<sub>50</sub> of 0.87 nM was determined. In addition, no effects of cs-130<sup>T102Y/Q113F/N114L</sup>Fc and its monomeric form cs-130<sup>T102Y/Q113F/N114L</sup> were observed on IL-11 trans-signaling or IL-6 classic-signaling-induced proliferation at any concentration (up to 100 nmol/L) (Fig. 6B and fig. S4).

### ***cs-130Fc variants inhibit T<sub>H</sub>17 cell formation in a dose-dependent manner***

IL-6 trans-signaling mediated expansion of T<sub>H</sub>17 cells is a crucial factor in the pathology of a variety of autoimmune diseases including rheumatoid arthritis (3). Inflammation results in reduced surface expression of IL-6R on activated T<sub>H</sub> (CD4<sup>+</sup>CD<sup>44hi</sup>CD<sup>62Llo</sup>) cells (32) and T cell activation is linked with a downregulation of IL-6R (33, 34). Activated neutrophils, monocytes and T cells can release soluble IL-6R through IL-6R shedding (33, 35-37) leading to an increase in local soluble IL-6R levels. The increased sIL-6R levels enable IL-6 trans-signaling mediated activation of cells lacking surface IL-6R. In line with this, IL-6 trans-signaling promotes the local expansion of T helper 17 (T<sub>H</sub>17) cells, which in turn can be inhibited by the IL-6 trans-signaling inhibitor sgp130Fc (32).

Because we observed that cs-130Fc variants efficiently blocked IL-6 trans-signaling without affecting IL-6 classic-signaling in the Ba/F3 test system, we next investigated whether they can also inhibit IL-6:sIL-6R induced T<sub>H</sub>17 expansion. To assess the effect of cs-130Fc variants on T<sub>H</sub>17 expansion, naive CD4<sup>+</sup> T-cells from *IL6ra*<sup>-/-</sup> mice were treated using a combination of IL-6 and sIL-6R, transforming growth factor (TGF)β, antibodies to IL-2 and IL-23 alongside stimulation with antibodies to CD3/CD28. T<sub>H</sub>17 cell expansion was monitored by flow cytometry based on IL-17 production (Fig. 7 and fig. S5). sgp130Fc, cs-130Fc and cs-130 displayed comparable inhibition of T<sub>H</sub>17 cell expansion. With similar IC<sub>50</sub> values, sgp130Fc and cs-130Fc were equally potent, while sgp130Fc was twice as active as cs-130. During control experiments using c<sub>GFP</sub>S-130Fc and cs-130<sup>190K/F191E</sup>Fc no effect on T<sub>H</sub>17 expansion was observed. In addition to T<sub>H</sub>17 expansion, we also monitored the effect of inhibitory proteins on the secretion of IL-17 (fig. S6). To this end, IL-17 secreted by T cells treated with increasing inhibitor concentrations as described above for cell expansion assays was quantified by ELISA. We observed very similar IC<sub>50</sub> values for sgp130Fc, cs-130Fc and cs-130 with regards to their inhibition of IL-17 secretion.

## **Discussion**

IL-6 trans-signaling is heavily associated with chronic inflammatory processes (40). For IL-11 signaling, the picture is much less clear. Soluble IL-11R is present in human serum (18). Like the related IL-6R, the IL-11R can be shed from the cell surface by ADAM10 (18). In

analogy to IL-6, IL-11 can induce trans-signaling (18, 41, 42). Yet, in contrast to IL-6, the physiological role of IL-11 trans-signaling is completely unknown.

For our understanding of IL-6 biology, sgp130Fc had a significant impact. Using sgp130Fc transgenic mice, a crucial role of IL-6 trans-signaling on e.g. overall inflammatory processes (43), cardiac fibrosis (44), inflammatory bowel disease, lupus erythematosus, cancer, pulmonary emphysema, endotoxemia, overall IL-6 signaling in the brain [all reviewed in (45)] has been demonstrated. In addition, a plethora of studies utilizing injections of recombinant sgp130Fc in murine disease models contributed to the knowledge on the physiological and pathophysiological impact of IL-6 trans-signaling [reviewed in (45)]. Other members of the IL-6 family of cytokines including CNTF, CLC, OSM, CT-1, LIF, IL-27 and IL-11 also induce signal transduction via gp130. Thus, sgp130Fc may have an influence on signaling induced by other IL-6 family members. Especially IL-11-mediated effects have to be considered, since IL-11, like IL-6, forms a ternary complex composed of cytokine,  $\alpha$ -receptor and gp130, leading to gp130 dimerization and subsequent signal transduction. sgp130Fc is a potent inhibitor of IL-11 trans- and cluster-signaling (13, 18, 46). Consequently, the dissection of IL-6 and IL-11 trans-signaling effects by sgp130Fc is a complicated endeavor. It cannot be excluded that phenotypes observed in sgp130Fc models stem from combined effects on IL-6 and IL-11 signaling. IL-11 is a multifunctional cytokine with effects on hepatocytes, B-cells, macrophages, osteoclasts, cardiac myocytes and fibroblast hematopoietic cells including functions in cardiac regeneration and fibrosis, colon regeneration, bone metabolism and cancer (47, 48). Thus, effects on IL-11 signal transduction need to be considered when sgp130Fc is utilized to investigate or modulate IL-6 trans-signaling. Here we describe IL-6 selective chimeric soluble gp130 variants with strongly reduced or absent effects on IL-11 trans-signaling. These novel tools can greatly simplify the analysis of IL-6- and IL-11-specific trans-signaling phenotypes.

IL-6 is an important drug target, and many therapeutic strategies have been developed to inhibit excessive IL-6 signaling. These include molecules incorporating inactivated cytokines (49), receptor fusion proteins (50) and monoclonal antibodies (28, 51, 52). Several monoclonal antibodies directed against IL-6 or its  $\alpha$ -receptor are approved for therapeutic applications. All the aforementioned molecules act as competitive inhibitors through binding to IL-6 or the IL-6R. Hence, none of these inhibitors is able to differentiate between IL-6 classic and trans-signaling, since both pathways utilize the extracellular domains of IL-6 and the IL-6R. Thus, all therapeutic anti-IL-6 approaches have suffered from side effects, including impaired innate immune response against bacterial pathogens due to defective IL-6 classic-signaling (17). Several different endogenous soluble isoforms of gp130, implicated in the regulation of IL-6-type cytokine signal transduction, have been detected in human serum (22, 51, 53, 54). sgp130Fc is an IL-6 signaling inhibitor that is mostly restricted to the trans-signaling pathway (20), and sgp130Fc treatment does not result in impaired bacterial control in mouse models of *L. monocytogenes* infection (17). sgp130Fc is considered a potential therapeutic molecule for the treatment of IL-6 trans-signaling related diseases. The sgp130Fc variant olamkcept successfully completed a phase IIa trial in Crohn's disease (CD) and ulcerative colitis (UC) (EudraCT: 2016-

000205-36) (55) with promising outcomes including complete remission in 22% of the UC and 14% of the CD patients and a clinical response in 44% of the UC and 55% of the CD patients, respectively.

In this study, we generated size-reduced variants of sgp130Fc with improved activity and selectivity for IL-6 trans-signaling. For antibodies, an inverse correlation between tissue penetration and molecular weight has been shown (24). The large size of sgp130Fc may limit its tissue penetration. Smaller variants of sgp130Fc have been characterized regarding their inhibitory profiles, but all of them have decreased inhibitory activities (20, 22, 25). To reconstitute sgp130Fc-like activity in cs-130Fc variants, domains D1-D3 of sgp130 were fused to a sdAb recognizing the IL-6/sIL-6R complex. The resulting fusion proteins demonstrated comparable and, for some, even improved IL-6 trans-signaling inhibition compared to sgp130Fc. Furthermore, we could demonstrate that dimeric cs-130Fc and monomeric cs-130 had reduced or no effects on IL-11 trans-signaling while sgp130Fc potently inhibited IL-11 trans-signaling. Olamkicept induces minor adverse effects including upper respiratory infections, recurrence of herpes labialis and skin and subcutaneous disorders (55). In addition, differences in the transcriptional signature in response to olamkicept or anti-IL-6R treatment were described. Differential activities of olamkicept and IL-6R antibodies were attributed to differences in the downstream effects of IL-6 classic and trans-signaling and to possible effects of olamkicept on other gp130 dependent trans-signaling events as IL-11 signaling. Hence, the described IL-6 trans-signaling selectivity may be an important step towards therapeutically relevant sgp130 variants with reduced adverse effects.

sgp130Fc has been described to inhibit IL-6-mediated T<sub>H</sub>17 cell expansion in disease models of rheumatoid arthritis (56). In line with these findings, we observed an inhibitory effect of cs-130 variants rivaling the effect of sgp130Fc in T<sub>H</sub>17 cell expansion assays. However, because of its improved binding kinetics, decreased size and IL-11 reactivity, we suggest that cs-130Fc and cs130 may be superior to sgp130Fc in terms of pharmacological inhibition of T<sub>H</sub>17 cell formation.

sgp130Fc was optimized in the past to improve stability and binding affinities for IL-6 (27). Mutations at IL-6 binding sites II and III were described to improve binding affinities towards IL-6 resulting in improved activity (27). We show that incorporation of mutations at site III of sgp130Fc abrogates its effects on IL-11, while the inhibitory activity towards IL-6 trans-signaling is improved. Incorporation of these mutations in cs-130<sup>T102Y/Q113F/N114L</sup>Fc variants resulted in further improvement of IL-6 trans-signaling inhibition and reduced cross-reactivity with IL-11 signaling.

In summary, we report miniaturized fusion proteins displaying comparable and, for some, even improved IL-6 trans-signaling inhibition compared to sgp130Fc, while at the same time no effects on IL-11 trans-signaling were observed. These proteins may be beneficial for the physiological and pathophysiological dissection of IL-6 family cytokine signaling modes.

Furthermore, there are possible therapeutic applications of cs-130Fc variants due to their selective inhibition of IL-6 trans-signaling and relatively small size.

## Materials and Methods

### *Cloning of cs-130Fc variants*

The cDNA encoding single domain antibody VHH6 was chemically synthesized by Biocat (Heidelberg, Germany). VHH6 was subsequently subcloned in pcDNA3.1-nHyper-IL-6-Fc (13) to generate pcDNA3.1-IL-6-VHH6-Fc. Domains D1-D3 of sgp130Fc were PCR-amplified using the following oligonucleotides: D1-D3 fw: AAGCTTGCCACCATGCTGACC, D1-D3 rv: CTCGAGCTTAGAGGGTCTGTCCTCGTAGG, D2 fw SOE: GATATGTGGAAAAGACATTTCTTCTGGACTGCCCCCGAGAAGCCCAAG, Delta D1 rvSOE: CAGGTTTAGCAGCGGCGGC, D1 rv: CTCGAGGCCGCTGATGATTGTGATGCC. Amplicons were subcloned via HindIII and XhoI sites to generate pcDNA3.1-cs-130Fc. An expression plasmid for c<sub>GFPs</sub>-130Fc was generated by fusion of coding sequences of the D1-D3 domains of sgp130 with cDNA encoding a nanobody against GFP (57). The resulting pcDNA3.1-c<sub>GFPs</sub>-130 was used to subclone c<sub>GFPs</sub>-130 via HindIII and NotI sites into pcDNA3.1-cs-130Fc to generate c<sub>GFPs</sub>-130Fc. The inactivating mutations Y190K/F191E or the activity-boosting mutations T102Y/Q113F/N114L were introduced into pcDNA3.1-cs-130Fc via site directed mutagenesis using the following oligonucleotides: gp130<sup>Y190K/F191E</sup> rv: ACCCACACTTCGATGTTACCTCCTTCACGGTGCTGTAGTCCACGG, gp130<sup>Y190K/F191E</sup> fw: CCGTGGACTACAGCACCGTGAAGGAGGTGAACATCGAAGTGTGGGT, T102Yfw: CAG CCTGAACATCCAGCTGTATTGCAACATCCTGACCTTCG, T02Yrv: CGAAGGTCAGGA TGTTGCAATACAGCTGGATGTTCAAGGCTG, Q113F/N114Lfw: GCTGATGATTGTGATGCCGTACACTAGGAATTCAGCTGGCCGAAGGTCAGGATG, Q113F/N114Lrv: CATCCTGACCTTCGGCCAGCTGGAATTCCTAGTGTACGGCATCACAATCATCAGC.

### *Cells and reagents*

The generation of Ba/F3-gp130 and Ba/F3-gp130-IL-6R cells has been described elsewhere (58). Ba/F3 cell lines were grown in DMEM high glucose culture medium (GIBCO<sup>®</sup>, Life Technologies, Darmstadt, Germany) supplemented with 10% fetal bovine serum (GIBCO<sup>®</sup>, Life Technologies), 60 mg/l penicillin and 100 mg/l streptomycin (Genaxxon bioscience GmbH, Ulm, Germany) at 37°C with 5% CO<sub>2</sub>. Proliferation of Ba/F3-gp130 cells was maintained in the presence of hyper-IL-6 (H-IL-6), a fusion protein of IL-6 and sIL-6R, which mimics the IL-6 trans-signaling complex (59). Expression and purification of human hyper-IL-6 and human IL-6 was performed as described previously (59). Antibodies directed against STAT3 phosphorylated at Tyr<sup>705</sup> (clone D3A7) and STAT3 (clone 124H6) were obtained from Cell Signaling Technology (Frankfurt, Germany). Rabbit anti-human IgG Fc (#31423) and peroxidase-conjugated secondary mAbs (#31432, #31462) were obtained from Pierce (Thermo Fisher Scientific, Waltham, MA, USA). Antibodies directed against pERK (#4370) and ERK (#4695)

were obtained from Cell Signaling. Recombinant sgp130Fc and IL-6 were produced and purified as described previously (60). Rabbit anti-human IgG Fc HRP conjugate was obtained from Thermo Fisher Scientific (Waltham, MA, USA). Recombinant soluble sgp130<sup>T102Y/Q113F/N114L</sup>-Fc and sIL-6R were obtained from CONARIS Research Institute AG (Kiel, Germany). An expression plasmid for IL-11( $\Delta$ 11)His<sub>6</sub> lacking the first 11 amino acids of IL-11, was kindly provided by Prof. Dr. Christoph Garbers (Otto-von-Guericke-University Magdeburg). IL-11 was expressed as a soluble protein in *E. coli* and purified via immobilized metal affinity chromatography. The sIL-11R was obtained from Bio-Techne (Wiesbaden, Germany).

#### *Transfection, transduction and selection of cells*

CHO-K1 cells were cultured in DMEM medium. For expression of recombinant proteins,  $5 \times 10^5$  CHO-K1 cells were transfected with Turbofect (Thermo Fisher Scientific, Waltham, MA, USA) and 5  $\mu$ g plasmid DNA encoding cs-130Fc variants. At 5 hours after transfection, the medium was exchanged to DMEM medium without transfection reagent. For the generation of stable CHO-K1 cell lines, G418 was added to the medium 48 hours after transfection. Single clones were selected via limiting dilution. Positive clones expressing Fc fusion proteins were identified by Western blotting using anti-human Fc antibodies.

#### *Proliferation assays*

Ba/F3-gp130 and Ba/F3-gp130-IL-6R cells were washed and 5,000 cells of each cell line were cultured for three days in a final volume of 100  $\mu$ l in the presence of cytokines and inhibitors. The CellTiter-Blue<sup>®</sup> Reagent was used to determine cellular viability by recording the fluorescence (excitation 560 nm, emission 590 nm) using an Infinite M200 PRO plate reader (Tecan, Crailsheim, Germany) immediately after adding 20  $\mu$ l of reagent per well (time point 0) and up to 120 min thereafter.

#### *Stimulation of Ba/F3 cells assays and lysate preparation*

$10^6$  Ba/F3-gp130 cells/ml and variants thereof were washed and starved in serum-free medium for 5 hours. Prior to stimulation, cytokines and inhibitors were preincubated at room temperature for 30 min. Subsequently, cells were stimulated with the indicated cytokines and inhibitor combinations for 30 min, harvested by centrifugation at 4°C for 5 min at 1500 x g, frozen and lysed. Protein concentration of cell lysates was determined by the BCA Protein Assay (Pierce, Thermo Scientific). Analysis of STAT3 activation was performed by Western blotting of 25–75  $\mu$ g of total protein from total cell lysates and subsequent detection steps using the anti-pSTAT3 (Tyr<sup>705</sup>) (1:1000) and anti-STAT3 (1:2000) antibodies described above.

#### *Western blotting*

Proteins were separated by SDS-PAGE and transferred to polyvinylidene difluoride (PVDF) or nitrocellulose membranes. Membranes were blocked and probed with the indicated primary antibodies. After washing, membranes were incubated with secondary peroxidase-conjugated antibodies or fluorescence-labeled secondary antibodies (1:10.000 dilution). The

Immobilon™ Western Reagents (Millipore Corporation, Billerica, MA, USA) and the ChemoCam Imager (INTAS Science Imaging Instruments GmbH, Göttingen, Germany) or the Odyssey Fc Imaging System (LI-CORE Biosciences, Bad Homburg, Germany) were used for signal detection. Control STAT3 blots were produced on the same membrane either following stripping or simultaneously to pSTAT3 imaging using the Odyssey Fc Imaging System.

### *Expression and purification of recombinant proteins*

Inhibitory proteins were produced in stably transfected CHO-K1 cells (see above) using a roller bottle system. Culture supernatants from roller bottles were harvested and centrifuged at  $1,000 \times g$  and  $4^\circ\text{C}$  for 30 min, followed by centrifugation of the resulting supernatant at  $10,000 \times g$  at  $4^\circ\text{C}$  for 30 min. The supernatant of the second centrifugation step was filtered (bottle top filter,  $0.45\text{-}\mu\text{m}$  pore diameter; Nalgene; Rochester, NY) and purified by affinity chromatography. Before chromatography, the pH values of the filtered cell culture supernatants were adjusted to 7.4. Supernatant was loaded on a protein-A column (HiTrap protein A HP; GE Healthcare) at a flow rate of 2 ml/min. The column was then washed with 30 column volumes of PBS. Proteins were eluted at pH 3.2-3.5 using a 50 mM citric acid buffer. Fractions of 1 ml were collected. Fractions containing the protein peak were pooled, and the pH was adjusted to pH 7 with 1 M Tris. Proteins were buffer exchanged to PBS using illustra NAP 25 (GE Healthcare Life Sciences, Munich, Germany) columns. Protein concentration was determined by measuring absorbance at 280 nm, and samples were flash-frozen in liquid nitrogen. Protein quality was assessed by SDS-PAGE and Coomassie staining. Following affinity purification, cs-130Fc variants were processed with TEV protease (ratio of protein:TEV protease of 1:10) overnight at  $4^\circ\text{C}$ . After protease processing, the resulting protein fragments were separated by size exclusion chromatography (gel filtration) using a Superdex® 200 Increase 10/300 GL column (GE Healthcare Life Sciences, Munich, Germany).

### *Surface plasmon resonance*

For surface plasmon resonance experiments, a Biacore X100 instrument (GE Healthcare Life Sciences) was used. Analysis was performed in single cycle mode using CM5 sensor chips. For every single experiment we used a new sensor chip because of the high affinity protein interaction which makes the regeneration of chips inefficient. Experiments were carried out at  $25^\circ\text{C}$  in HBS-P + buffer (GE-Healthcare), containing 10 mM HEPES, pH 7.4, 0.15 M NaCl, 0.05% (v/v) surfactant P20 (GE Healthcare). Hyper-IL-6-Fc or hyper-IL-11-Fc were immobilized by amine coupling on a CM5 chip (1200 RU). After immobilization, sgp130 and cs-130 variants were injected at a flow rate of  $30 \mu\text{l}/\text{min}$  at increasing concentrations (5–80 nM). Association of cs-130Fc variants in each defined concentration was monitored in periods of 60 sec, and the global dissociation was measured at the end of the final injection in periods of 600 sec. The final graphs were fitted using 1:1 binding model. Due to the complexity of the data obtained, as was also reported previously Adams *et al.* (23), and its extremely low dissociation rate constant, we have limited the kinetic characterization to the dissociation rate constant  $k_{\text{off}}$  where an obvious difference was observed. This is in accordance with the SPR analysis Adams *et al.* (23) performed on the interaction of an IL-6-sIL-6R fusion protein with the VHH6 sdAb that is part of cs-130Fc.

### *Size exclusion chromatography coupled to multi-angle light scattering (SEC-MALS)*

The determination of the absolute weight-averaged molar mass ( $M_w$ ) and its distribution was taken out using a Multi-Angle Light Scattering (MALS) system from Wyatt Technology. An 18-angle light scattering detector (model DAWN) and a refractive index detector (model Optilab T-rEX, Wyatt Technology) were coupled to an Agilent 1260 Infinity II HPLC system, consisting of a quaternary pump (model G7111B, incl. degasser), a variable wavelength detector (VWD, model G7114A) as well as an autosampler (model G7129A). Separation was achieved using a GE Superose 6 Increase column with a flow rate of 0.5 mL/min. PBS (pH 7.0) was used as the mobile phase. Between 10 and 50  $\mu$ g were injected per sample. The control of the HPLC and the analysis of the light scattering as well as the concentration data were carried out using the software ASTRA 7 from Wyatt Technology. Measurements were performed by representatives of Wyatt Technology.

### *In vitro T cell cultures*

Murine CD4<sup>+</sup> T-cells were enriched by negative magnetic selection (Miltenyi Biotec) before purification of naïve (CD4<sup>+</sup>CD25<sup>-</sup>CD44<sup>lo</sup>CD62L<sup>hi</sup>) T-cells. T-cell purity was > 92%. Naïve CD4<sup>+</sup> T-cells were cultured in IMDM medium already containing 4 mM L-glutamine and 25 mM HEPES and supplemented with 10% (v/v) FBS, 100 U/mL penicillin, 100 mg/mL streptomycin, and 50 mM  $\beta$ -mercaptoethanol (all from Thermo Fisher Scientific).  $1.5 \times 10^5$  CD4<sup>+</sup> T cells were cultured in 96-well U-shape bottom plates coated with anti-CD3 (1 mg/mL; 145-2C11), added the previous day and incubated at 4°C overnight, and soluble anti-CD28 (5 mg/mL; 37.51). Recombinant mouse cytokines were included at the following concentrations to promote differentiation of naïve CD4<sup>+</sup> T-cells into a defined T<sub>H</sub>17 lineage: TGF- $\beta$  (1 ng/mL), IL-23 (20 ng/mL), IL-6 (50 ng/mL), sIL-6R (100 ng/mL) and anti-IL-2 (10 ng/mL). Increasing inhibitor concentrations were added as indicated.  $1.5 \times 10^5$  cells were plated and grown at 37°C with 5% CO<sub>2</sub> for 4 days before phenotypic characterisation of 40000 cells by flow cytometry.

### *Animals*

C57BL/6 IL-6 receptor-deficient mice (*CD126<sup>-/-</sup>*) have been described previously and were bred under approved UK Home Office guidelines in Cardiff University (32). All mice were 8 to 12 weeks of age.

### *Flow cytometry*

For intracellular cytokine staining (ICS), cells were cultured with 50 ng PMA (phorbol 12-myristat-13-acetate), 500 ng ionomycin and 3 mM monensin (all from Sigma-Aldrich) for 4 hours prior to flow cytometry analysis (7,8,15). Prior to immune-labelling, cells were treated with Fc block (BD Biosciences) to reduce nonspecific Ab binding. Cells were stained for cell surface markers, then fixed and permeabilised in Cytofix/Cytoperm (BD Biosciences) before intracellular detection of cytokines. Flow cytometric analysis of cells was performed using Zombie Aqua live/dead stain (BioLegend), anti-CD4 (RM4-5), anti-IFN- $\gamma$  (XMG 1.2), and anti-IL-17 (TC11-18H.1). Cell reads were acquired using a FACSCanto II flow cytometer using

FACSDiva software (BD Biosciences). Data analysis was conducted using FlowJo Version 10.7.1 (Tree Star Inc, US).

### *Cell culture supernatants measurement of IL-17A*

IL-17A levels were quantified in cell culture supernatants using a commercial murine IL-17A (Duoset kits from R&D Systems).

### *Statistical analysis*

For proliferation assays, a representative experiment of  $n \geq 3$  assays with comparable results is displayed.  $IC_{50}$  values were calculated using a non-linear regression analysis in GraphPad Prism 6.0 (version 6.00 for Windows, GraphPad Software, La Jolla California USA, www.graphpad.com”) from 3 individual experiments. Quantification of Western blot data was performed using Image studio lite Vers. 5.2 (Li-COR) for  $n \geq 3$  individual experiments. Resulting intensities were normalized to positive controls. For multiple comparisons, one-way ANOVA, followed by Dunnett’s correction, was used (GraphPad Prism 6.0). Statistical significance was set at the level of  $p < 0.05$ .  $T_H17$  cell data are presented as percentage inhibition normalized to controls. Means of 3 replicates  $\pm$  SD for flow cytometry are displayed. A non-linear regression was used to fit a dose response curve to determine the inhibitors  $IC_{50}$  using GraphPad Prism 7 software (version 7.00 for Windows, GraphPad Software, La Jolla California USA, www.graphpad.com”).

## **Supplementary Materials**

Figures S1 – S6

## **References and Notes**

1. J. Scheller, A. Chalaris, D. Schmidt-Arras, S. Rose-John, The pro- and anti-inflammatory properties of the cytokine interleukin-6. *Biochim Biophys Acta* **1813**, 878-888 ( 2011) .
2. J. Scheller, C. Garbers, S. Rose-John, Interleukin-6: from basic biology to selective blockade of pro-inflammatory activities. *Semin Immunol* **26**, 2-12 ( 2014) .
3. T. Alonzi, E. Fattori, D. Lazzaro, P. Costa, L. Probert, G. Kollias, F. De Benedetti, V. Poli, G. Ciliberto, Interleukin 6 is required for the development of collagen-induced arthritis. *J Exp Med* **187**, 461-468 ( 1998) .
4. S. Ohshima, Y. Saeki, T. Mima, M. Sasai, K. Nishioka, S. Nomura, M. Kopf, Y. Katada, T. Tanaka, M. Suemura, T. Kishimoto, Interleukin 6 plays a key role in the development of antigen-induced arthritis. *Proc Natl Acad Sci U S A* **95**, 8222-8226 ( 1998) .

5. E. B. Samoilova, J. L. Horton, B. Hilliard, T. S. Liu, Y. Chen, IL-6-deficient mice are resistant to experimental autoimmune encephalomyelitis: roles of IL-6 in the activation and differentiation of autoreactive T cells. *J Immunol* **161**, 6480-6486 ( 1998) .
6. R. Atreya, M. F. Neurath, Involvement of IL-6 in the pathogenesis of inflammatory bowel disease and colon cancer. *Clin Rev Allergy Immunol* **28**, 187-196 ( 2005) .
7. J. S. Hyams, J. E. Fitzgerald, W. R. Treem, N. Wyzga, D. L. Kreutzer, Relationship of functional and antigenic interleukin 6 to disease activity in inflammatory bowel disease. *Gastroenterology* **104**, 1285-1292 ( 1993) .
8. R. Atreya, J. Mudter, S. Finotto, J. Mullberg, T. Jostock, S. Wirtz, M. Schutz, B. Bartsch, M. Holtmann, C. Becker, D. Strand, J. Czaja, J. F. Schlaak, H. A. Lehr, F. Autschbach, G. Schurmann, N. Nishimoto, K. Yoshizaki, H. Ito, T. Kishimoto, P. R. Galle, S. Rose-John, M. F. Neurath, Blockade of interleukin 6 trans signaling suppresses T-cell resistance against apoptosis in chronic intestinal inflammation: evidence in crohn disease and experimental colitis in vivo. *Nat Med* **6**, 583-588 ( 2000) .
9. M. R. Schneider, A. Hoefflich, J. R. Fischer, E. Wolf, B. Sordat, H. Lahm, Interleukin-6 stimulates clonogenic growth of primary and metastatic human colon carcinoma cells. *Cancer Lett* **151**, 31-38 ( 2000) .
10. C. Becker, M. C. Fantini, C. Schramm, H. A. Lehr, S. Wirtz, A. Nikolaev, J. Burg, S. Strand, R. Kiesslich, S. Huber, H. Ito, N. Nishimoto, K. Yoshizaki, T. Kishimoto, P. R. Galle, M. Blessing, S. Rose-John, M. F. Neurath, TGF-beta suppresses tumor progression in colon cancer by inhibition of IL-6 trans-signaling. *Immunity* **21**, 491-501 ( 2004) .
11. S. Grivennikov, E. Karin, J. Terzic, D. Mucida, G. Y. Yu, S. Vallabhapurapu, J. Scheller, S. Rose-John, H. Cheroutre, L. Eckmann, M. Karin, IL-6 and Stat3 are required for survival of intestinal epithelial cells and development of colitis-associated cancer. *Cancer Cell* **15**, 103-113 ( 2009) .
12. S. Heink, N. Yogev, C. Garbers, M. Herwerth, L. Aly, C. Gasperi, V. Husterer, A. L. Croxford, K. Moller-Hackbarth, H. S. Bartsch, K. Sotlar, S. Krebs, T. Regen, H. Blum, B. Hemmer, T. Misgeld, T. F. Wunderlich, J. Hidalgo, M. Oukka, S. Rose-John, M. Schmidt-Supprian, A. Waisman, T. Korn, Trans-presentation of IL-6 by dendritic cells is required for the priming of pathogenic TH17 cells. *Nat Immunol* **18**, 74-85 ( 2017) .

13. L. Lamertz, F. Rummel, R. Polz, P. Baran, H.-S. Signal ; Soluble gp130 prevent interleukin-6 and interleukin-11 cluster signaling but not intracellular autocrine responses. *Sci. Signal* ; ( 2018) .
14. V. R. Lang, M. Englbrecht, J. Rech, H. Nusslein, K. Manger, F. Schuch, H. P. Tony, M. Fleck, B. Manger, G. Schett, J. Zwerina, Risk of infections in rheumatoid arthritis patients treated with tocilizumab. *Rheumatology ( Oxford)* **51**, 852-857 ( 2012) .
15. R. A. LeBlanc, L. Pesnicak, E. S. Cabral, M. Godleski, S. E. Straus, Lack of interleukin-6 ( IL-6) enhances susceptibility to infection but does not alter latency or reactivation of herpes simplex virus type 1 in IL-6 knockout mice. *J Virol* **73**, 8145-8151 ( 1999) .
16. C. Garbers, W. Thaiss, G. W. Jones, G. H. Waetzig, I. Lorenzen, F. Guilhot, R. Lissilaa, W. G. Ferlin, J. Grotzinger, S. A. Jones, S. Rose-John, J. Scheller, Inhibition of classic signaling is a novel function of soluble glycoprotein 130 ( sgp130) , which is controlled by the ratio of interleukin 6 and soluble interleukin 6 receptor. *J Biol Chem* **286**, 42959-42970 ( 2011) .
17. J. Hoge, I. Yan, N. Janner, V. Schumacher, A. Chalaris, O. M. Steinmetz, D. R. Engel, J. Scheller, S. Rose-John, H. W. Mittrucker, IL-6 controls the innate immune response against *Listeria monocytogenes* via classical IL-6 signaling. *J Immunol* **190**, 703-711 ( 2013) .
18. J. Lokau, R. Nitz, M. Agthe, N. Monhasery, S. Aparicio-Siegmund, N. Schumacher, J. Wolf, K. Moller-Hackbarth, G. H. Waetzig, J. Grotzinger, G. Muller-Newen, S. Rose-John, J. Scheller, C. Garbers, Proteolytic Cleavage Governs Interleukin-11 Trans-signaling. *Cell Rep* **14**, 1761-1773 ( 2016) .
19. W. Hui, M. Bell, G. Carroll, Soluble glycoprotein 130 ( gp130) attenuates OSM- and LIF-induced cartilage proteoglycan catabolism. *Cytokine* **12**, 151-155 ( 2000) .
20. T. Jostock, J. Müllberg, S. Ozbek, R. Atreya, G. Blinn, N. Voltz, M. Fischer, M. F. Neurath, S. Rose-John, Soluble gp130 is the natural inhibitor of soluble interleukin-6 receptor transsignaling responses. *European journal of biochemistry / FEBS* **268**, 160-167 ( 2001) .
21. M. Lin, S. Rose-John, J. Grotzinger, U. Conrad, J. Scheller, Functional expression of a biologically active fragment of soluble gp130 as an ELP-fusion protein in transgenic plants: purification via inverse transition cycling. *Biochem J* **398**, 577-583 ( 2006) .
22. J. Sommer, C. Garbers, J. Wolf, A. Trad, J. M. Moll, M. Sack, R. Fischer, J. Grotzinger, G. H. Waetzig, D. M. Floss, J. Scheller, Alternative intronic polyadenylation generates

- the interleukin-6 trans-signaling inhibitor sgp130-E10. *J Biol Chem* **289**, 22140-22150 ( 2014) .
23. R. Adams, R. J. Burnley, C. R. Valenzano, O. Qureshi, C. Doyle, S. Lumb, M. Del Carmen Lopez, R. Griffin, D. McMillan, R. D. Taylor, C. Meier, P. Mori, L. M. Griffin, U. Wernery, J. Kinne, S. Rapecki, T. S. Baker, A. D. Lawson, M. Wright, A. Ettore, Discovery of a junctional epitope antibody that stabilizes IL-6 and gp80 protein:protein interaction and modulates its downstream signaling. *Scientific reports* **7**, 37716 ( 2017) .
  24. Z. Li, B. F. Krippendorff, S. Sharma, A. C. Walz, T. Lave, D. K. Shah, Influence of molecular size on tissue distribution of antibody fragments. *MAbs* **8**, 113-119 ( 2016) .
  25. P. J. Richards, M. A. Nowell, S. Horiuchi, R. M. McLoughlin, C. A. Fielding, S. Grau, N. Yamamoto, M. Ehrmann, S. Rose-John, A. S. Williams, N. Topley, S. A. Jones, Functional characterization of a soluble gp130 isoform and its therapeutic capacity in an experimental model of inflammatory arthritis. *Arthritis Rheum* **54**, 1662-1672 ( 2006) .
  26. I. Kurth, U. Horsten, S. Pflanz, H. Dahmen, A. Kuster, J. Grotzinger, P. C. Heinrich, G. Muller-Newen, Activation of the signal transducer glycoprotein 130 by both IL-6 and IL-11 requires two distinct binding epitopes. *J Immunol* **162**, 1480-1487 ( 1999) .
  27. S. Tenhumberg, G. H. Waetzig, A. Chalaris, B. Rabe, D. Seegert, J. Scheller, S. Rose-John, J. Grötzinger, Structure-guided Optimization of the Interleukin-6 Trans-signaling Antagonist sgp130. *Journal of Biological Chemistry* **283**, 27200-27207 ( 2008) .
  28. N. Nishimoto, K. Yoshizaki, N. Miyasaka, K. Yamamoto, S. Kawai, T. Takeuchi, J. Hashimoto, J. Azuma, T. Kishimoto, Treatment of rheumatoid arthritis with humanized anti-interleukin-6 receptor antibody: a multicenter, double-blind, placebo-controlled trial. *Arthritis Rheum* **50**, 1761-1769 ( 2004) .
  29. K. Sato, M. Tsuchiya, J. Saldanha, Y. Koishihara, Y. Ohsugi, T. Kishimoto, M. M. Bendig, Reshaping a human antibody to inhibit the interleukin 6-dependent tumor cell growth. *Cancer Res* **53**, 851-856 ( 1993) .
  30. M. J. Boulanger, D.-c. C. Chow, E. E. Brevnova, K. C. Garcia, Hexameric structure and assembly of the interleukin-6/IL-6 alpha-receptor/gp130 complex. *Science ( New York, N.Y.)* **300**, 2101-2104 ( 2003) .
  31. M. Ehlers, J. Grotzinger, M. Fischer, H. K. Bos, J. P. Brakenhoff, S. Rose-John, Identification of single amino acid residues of human IL-6 involved in receptor binding and signal initiation. *J Interferon Cytokine Res* **16**, 569-576 ( 1996) .

32. G. W. Jones, R. M. McLoughlin, V. J. Hammond, C. R. Parker, J. D. Williams, R. Malhotra, J. Scheller, A. S. Williams, S. Rose-John, N. Topley, S. A. Jones, Loss of CD4<sup>+</sup> T cell IL-6R expression during inflammation underlines a role for IL-6 trans signaling in the local maintenance of Th17 cells. *J Immunol* **184**, 2130-2139 ( 2010) .
33. E. M. Briso, O. Dienz, M. Rincon, Cutting edge: soluble IL-6R is produced by IL-6R ectodomain shedding in activated CD4 T cells. *J Immunol* **180**, 7102-7106 ( 2008) .
34. N. D. Savage, S. H. Harris, A. G. Rossi, B. De Silva, S. E. Howie, G. T. Layton, J. R. Lamb, Inhibition of TCR-mediated shedding of L-selectin ( CD62L) on human and mouse CD4<sup>+</sup> T cells by metalloproteinase inhibition: analysis of the regulation of Th1/Th2 function. *Eur J Immunol* **32**, 2905-2914 ( 2002) .
35. S. M. Hurst, T. S. Wilkinson, R. M. McLoughlin, S. Jones, S. Horiuchi, N. Yamamoto, S. Rose-John, G. M. Fuller, N. Topley, S. A. Jones, Il-6 and its soluble receptor orchestrate a temporal switch in the pattern of leukocyte recruitment seen during acute inflammation. *Immunity* **14**, 705-714 ( 2001) .
36. R. M. McLoughlin, S. M. Hurst, M. A. Nowell, D. A. Harris, S. Horiuchi, L. W. Morgan, T. S. Wilkinson, N. Yamamoto, N. Topley, S. A. Jones, Differential regulation of neutrophil-activating chemokines by IL-6 and its soluble receptor isoforms. *J Immunol* **172**, 5676-5683 ( 2004) .
37. R. M. McLoughlin, J. Witowski, R. L. Robson, T. S. Wilkinson, S. M. Hurst, A. S. Williams, J. D. Williams, S. Rose-John, S. A. Jones, N. Topley, Interplay between IFN-gamma and IL-6 signaling governs neutrophil trafficking and apoptosis during acute inflammation. *J Clin Invest* **112**, 598-607 ( 2003) .
38. H. C. Reinecker, M. Steffen, T. Witthoef, I. Pflueger, S. Schreiber, R. P. MacDermott, A. Raedler, Enhanced secretion of tumour necrosis factor-alpha, IL-6, and IL-1 beta by isolated lamina propria mononuclear cells from patients with ulcerative colitis and Crohn's disease. *Clin Exp Immunol* **94**, 174-181 ( 1993) .
39. J. Mudter, M. F. Neurath, Apoptosis of T cells and the control of inflammatory bowel disease: therapeutic implications. *Gut* **56**, 293-303 ( 2007) .
40. S. Rose-John, IL-6 trans-signaling via the soluble IL-6 receptor: importance for the pro-inflammatory activities of IL-6. *Int J Biol Sci* **8**, 1237-1247 ( 2012) .
41. H. Dams-Kozłowska, K. Gryśka, E. Kwiatkowska-Borowczyk, D. Izycki, S. Rose-John, A. Mackiewicz, A designer hyper interleukin 11 ( H11) is a biologically active cytokine. *BMC Biotechnol* **12**, 8 ( 2012) .

42. S. Pflanz, I. Tacke, J. Grotzinger, Y. Jacques, S. Minvielle, H. Dahmen, P. C. Heinrich, G. Muller-Newen, A fusion protein of interleukin-11 and soluble interleukin-11 receptor acts as a superagonist on cells expressing gp130. *FEBS Lett* **450**, 117-122 ( 1999) .
43. B. Rabe, A. Chalaris, U. May, G. H. Waetzig, D. Seeger, A. S. Williams, S. A. Jones, S. Rose-John, J. Scheller, Transgenic blockade of interleukin 6 transsignaling abrogates inflammation. *Blood* **111**, 1021-1028 ( 2008) .
44. C. H. Chou, C. S. Hung, C. W. Liao, L. H. Wei, C. W. Chen, C. T. Shun, W. F. Wen, C. H. Wan, X. M. Wu, Y. Y. Chang, V. C. Wu, K. D. Wu, Y. H. Lin, T. S. Group, IL-6 transsignalling contributes to aldosterone-induced cardiac fibrosis. *Cardiovasc Res* **114**, 690-702 ( 2018) .
45. C. Garbers, S. Rose-John, Dissecting Interleukin-6 Classic- and Trans-Signaling in Inflammation and Cancer. *Methods Mol Biol* **1725**, 127-140 ( 2018) .
46. J. M. Moll, M. Wehmoller, N. C. Frank, L. Homey, P. Baran, C. Garbers, L. Lamertz, J. H. Axelrod, E. Galun, H. D. Mootz, J. Scheller, Split( 2) Protein-Ligation Generates Active IL-6-Type Hyper-Cytokines from Inactive Precursors. *ACS Synth Biol* **6**, 2260-2272 ( 2017) .
47. S. Schafer, S. Viswanathan, A. A. Widjaja, W. W. Lim, A. Moreno-Moral, D. M. DeLaughter, B. Ng, G. Patone, K. Chow, E. Khin, J. Tan, S. P. Chothani, L. Ye, O. J. L. Rackham, N. S. J. Ko, N. E. Sahib, C. J. Pua, N. T. G. Zhen, C. Xie, M. Wang, H. Maatz, S. Lim, K. Saar, S. Blachut, E. Petretto, S. Schmidt, T. Putoczki, N. Guimaraes-Camboa, H. Wakimoto, S. van Heesch, K. Sigmundsson, S. L. Lim, J. L. Soon, V. T. T. Chao, Y. L. Chua, T. E. Tan, S. M. Evans, Y. J. Loh, M. H. Jamal, K. K. Ong, K. C. Chua, B. H. Ong, M. J. Chakaramakkil, J. G. Seidman, C. E. Seidman, N. Hubner, K. Y. K. Sin, S. A. Cook, IL-11 is a crucial determinant of cardiovascular fibrosis. *Nature* **552**, 110-115 ( 2017) .
48. C. Garbers, J. Scheller, Interleukin-6 and interleukin-11: same same but different. *Biol Chem* **394**, 1145-1161 ( 2013) .
49. E. Sporeno, R. Savino, L. Ciapponi, G. Paonessa, A. Cabibbo, A. Lahm, K. Pulkki, R. X. Sun, C. Toniatti, B. Klein, G. Ciliberto, Human interleukin-6 receptor super-antagonists with high potency and wide spectrum on multiple myeloma cells. *Blood* **87**, 4510-4519 ( 1996) .

50. C. Ancey, A. Kuster, S. Haan, A. Herrmann, P. C. Heinrich, G. Muller-Newen, A fusion protein of the gp130 and interleukin-6Ralpha ligand-binding domains acts as a potent interleukin-6 inhibitor. *J Biol Chem* **278**, 16968-16972 ( 2003) .
51. J. G. Zhang, Y. Zhang, C. M. Owczarek, L. D. Ward, R. L. Moritz, R. J. Simpson, K. Yasukawa, N. A. Nicola, Identification and characterization of two distinct truncated forms of gp130 and a soluble form of leukemia inhibitory factor receptor alpha-chain in normal human urine and plasma. *J Biol Chem* **273**, 10798-10805 ( 1998) .
52. F. van Rhee, L. Fayad, P. Voorhees, R. Furman, S. Lonial, H. Borghaei, L. Sokol, J. Crawford, M. Cornfeld, M. Qi, X. Qin, J. Herring, C. Casper, R. Kurzrock, Siltuximab, a novel anti-interleukin-6 monoclonal antibody, for Castleman's disease. *J Clin Oncol* **28**, 3701-3708 ( 2010) .
53. M. Tanaka, M. Kishimura, S. Ozaki, F. Osakada, H. Hashimoto, M. Okubo, M. Murakami, K. Nakao, Cloning of novel soluble gp130 and detection of its neutralizing autoantibodies in rheumatoid arthritis. *J Clin Invest* **106**, 137-144 ( 2000) .
54. M. Narazaki, K. Yasukawa, T. Saito, Y. Ohsugi, H. Fukui, Y. Koishihara, G. D. Yancopoulos, T. Taga, T. Kishimoto, Soluble forms of the interleukin-6 signal-transducing receptor component gp130 in human serum possessing a potential to inhibit signals through membrane-anchored gp130. *Blood* **82**, 1120-1126 ( 1993) .
55. S. Schreiber, K. Aden, J. P. Bernardes, C. Conrad, F. Tran, H. Hoper, V. Volk, N. Mishra, J. I. Blase, S. Nikolaus, J. Bethge, T. Kuhbacher, C. Rocken, M. Chen, I. Cottingham, N. Petri, B. B. Rasmussen, J. Lokau, L. Lenk, C. Garbers, F. Feuerhake, S. Rose-John, G. H. Waetzig, P. Rosenstiel, Therapeutic Interleukin 6 Trans-signaling Inhibition by Olamkicept ( sgp130Fc) in Patients With Active Inflammatory Bowel Disease. *Gastroenterology*, ( 2021) .
56. M. Fujimoto, S. Serada, T. Naka, [Role of IL-6 in the development and pathogenesis of CIA and EAE]. *Nihon Rinsho Meneki Gakkai Kaishi* **31**, 78-84 ( 2008) .
57. E. Engelowski, A. Schneider, M. Franke, H. Xu, R. Clemen, A. Lang, P. Baran, C. Binsch, B. Knebel, H. Al-Hasani, J. M. Moll, D. M. Floss, P. A. Lang, J. Scheller, Synthetic cytokine receptors transmit biological signals using artificial ligands. *Nat Commun* **9**, 2034 ( 2018) .
58. A. Chalaris, B. Rabe, K. Paliga, H. Lange, T. Laskay, C. A. Fielding, S. A. Jones, S. Rose-John, J. Scheller, Apoptosis is a natural stimulus of IL6R shedding and contributes

- to the proinflammatory trans-signaling function of neutrophils. *Blood* **110**, 1748-1755 ( 2007) .
59. M. Fischer, J. Goldschmitt, C. Peschel, J. P. Brakenhoff, K. J. Kallen, A. Wollmer, J. Grotzinger, S. Rose-John, I. A bioactive designer cytokine for human hematopoietic progenitor cell expansion. *Nat Biotechnol* **15**, 142-145 ( 1997) .
60. N. F. Modares, R. Polz, F. Haghighi, L. Lamertz, K. Behnke, Y. Zhuang, C. Kordes, D. Haussinger, U. R. Sorg, K. Pfeffer, D. M. Floss, J. M. Moll, R. P. Piekorz, M. R. Ahmadian, P. A. Lang, J. Scheller, IL-6 trans-signaling controls liver regeneration after partial hepatectomy. *Hepatology*, ( 2019) .

**Acknowledgments:** SEC/MALS analysis was kindly provided by Dr. Deluweit and Dr. Mildner (Wyatt Technology). **Funding:** This work was supported by funding from the European Network on Noonan Syndrome and Related Disorders (NSEuroNet; grant number 01GM1621B to RA), and the Versus Arthritis Programme (grant 20770 to SA). **Author contributions:** DH and SH conducted most of the experiments. CD and AFB supported proliferation and stimulation experiments. MA performed the SPR experiments. ADS and SJ performed T-cell experiments. GHW, MRA, RD and JMM supported cloning, recombinant protein expression and purification, and cell culture. All authors helped writing the paper. JS and JMM designed the study, analyzed the data and wrote the paper. **Competing interests:** GHW is employed by CONARIS Research Institute AG (Kiel, Germany), which is commercially developing sgp130Fc proteins as therapeutics for inflammatory diseases, and is an inventor on the following intellectual property owned by CONARIS pertaining to the sgp130Fc used in the present study: Australian Patent No. 2007263939; Brazilian Patent Application No. PI0713063-5 (allowed); Canadian Patents No. 2,575,800, 2,656,440 and 2,702,982; Chinese Patent No. ZL200780024879.1; Eurasian Patent No. 015620; European Patents No. 1630232, 1873166 and 2212347; Indian Patent No. 265303; Japanese Patents No. 4615016, 5417171 and 5581214; South Korean Patent No. 10-1474817; Ukrainian Patent No. 95636; and U.S. Patents No. 8,206,948, 8,501,696, 8,895,012, 9,034,817, and 9,573,989. S.J. has provided consultancy for the following companies: Roche/Chugai (tocilizumab, Japan); Sanofi-Regeneron (sarilumab, USA and EU); Janssen, EUSA Pharma (siltuximab, EU); Ferring (olamkicept, EU); Mestag Therapeutics (M101 programme, EU); NovImmune SA (NI-1201; NI-101, CH), Eleven Biotherapeutics (EBI-031 programme, USA). J.M.M. and J.S. declare that they have applied for a patent that covers some of the molecules in the manuscript. All other authors declare that they have no competing or financial interests. **Data and materials availability:** All data needed to evaluate the conclusions in the paper are present in the paper or the Supplementary Materials.

## Figure legends

**Fig. 1.: Schematic illustration of cs-130Fc variant design.** (A) Domains D1-D3 (yellow) of sgp130Fc, incorporating sites II and III required for cytokine binding, were fused via a long flexible linker to a single domain antibody (VHH6) recognizing the complex of IL-6 and sIL-6R. A TEV protease recognition sequence connects VHH6 to the Fc fragment of a human IgG antibody. Due to the presence of the Fc fragment, all depicted proteins are disulfide linked dimers. Disulfide bonds connecting the Fc fragments are depicted as yellow lines. (B) Overview of different cs-130Fc variants. TEV protease recognition sequences ( | ) and positions of amino acid substitutions are indicated (\*). In both panels, protein domains are depicted as boxes, not size-proportional.

**Fig. 2: cs-130Fc variants are readily expressed and can be purified from CHO-K1 cells.** (A) CHO-K1 cells were transfected with expression plasmids encoding the displayed proteins. Cells were harvested and lysed 48 hours after transfection. Supernatants and lysates were analyzed by sodium dodecyl sulfate polyacrylamide gel electrophoresis (SDS-PAGE) and Western blotting using an antibody against human IgG-Fc. Western blots shown are representative of three different experiments with similar outcomes. (B) SDS-PAGE of purified sgp130Fc and cs-130Fc variants (10 µg of total protein) stained with Coomassie brilliant blue. (C) Following Fc affinity purification, cs-130Fc was processed with TEV protease, and the resulting protein fragments were separated via size exclusion chromatography (SEC). Three molecular species corresponding to different peaks observed (labeled 1-3) were isolated and analyzed by SDS-PAGE and Coomassie staining. BT, before TEV; PT, post TEV cleavage. (D) Coomassie staining of SDS-PAGE analysis of purified sgp130Fc and cs-130Fc variants. 5 µg total protein, non-reduced or reduced (Red. +), were loaded. (E) SEC-MALS analysis of affinity purified sgp130Fc and cs-130Fc variants. Between 10 and 50 µg were injected per sample on a Superpose 6 Increase column. Solid lines under the peaks correspond to molecular weight. (F) Conjugate analysis of cs-130Fc data from (E). Solid lines under the peak correspond to total mass (red), protein mass (black) and sugar mass (blue).

**Fig. 3: cs-130Fc variants are biologically active.** (A) Surface plasmon resonance analysis of hyper-IL-6-Fc binding to sgp130Fc and cs-130Fc variants. Hyper-IL-6-Fc was immobilized on a CM-5 chip and increasing concentrations of inhibitors were injected. Sensorgrams in response units (RU) over time are depicted as blue lines, global fit data are displayed as black lines. Residuals are shown below the sensorgrams. (B) A normalized overlay of the dissociation phases of sgp130Fc and cs-130Fc for their interaction with hyper-IL-6 for the highest concentration 80 nM is shown. (C) Ba/F3-gp130 cells were stimulated with 50 ng/ml IL-6 and 100 ng/ml sIL-6R in the presence of increasing sgp130Fc or cs-130Fc variant concentrations. At 72 hours after

stimulation, cellular proliferation was detected using a CellTiter-Blue assay. Normalization of relative proliferation was performed as described in Methods. Assays are representative of three independent experiments. **(D)** Western blot analysis of Ba/F3-gp130 cells stimulated for 30 min with 50 ng/ml IL-6 and 100 ng/ml sIL-6R (“+” lane) in the presence of the indicated concentrations of sgp130Fc, cs-130 or cs-130Fc variants. Unstimulated controls are indicated (“-” lane). Prior to stimulation, IL-6, sIL-6R and inhibitors were incubated separately for 30 min. Western blots were stained for phosphorylated (p)STAT3 and STAT3. Western blots are representative of three independent experiments. Normalized band intensity data are means  $\pm$  SD from all experiments.  $*P \leq 0.05$ ,  $**P \leq 0.01$ ,  $***P \leq 0.001$  and  $****P \leq 0.0001$  by analysis of variance (ANOVA) test with Dunnett’s correction.

**Fig. 4: cs-130Fc variants are poor inhibitors of IL-11 trans-signaling.** **(A)** Surface plasmon resonance analysis of hyper-IL-11-Fc binding to sgp130Fc and cs-130Fc variants. Hyper-IL-11-Fc was immobilized on a CM-5 chip and increasing concentrations of inhibitors were injected. Sensograms are depicted as blue lines, global fit data are displayed as black lines. **(B)** Ba/F3-gp130 cells were stimulated with 10 ng/ml IL-11 and 100 ng/ml sIL-11R in the presence of increasing sgp130Fc or cs-130Fc concentrations. At 72 hours after stimulation, cellular proliferation was detected using a CellTiter-Blue assay. Normalization of relative proliferation was performed as described in Methods. Assays are representative of three independent experiments. **(C)** Western blot analysis of Ba/F3-gp130 cells stimulated for 30 min with 10 ng/ml IL-11 and 100ng/ml sIL-11R (“+” lane) in the presence of the indicated concentrations of sgp130Fc or cs-130Fc variants. Unstimulated controls are indicated (“-” lane). Prior to stimulation, IL-11, sIL-11R and inhibitors were incubated for 30 min. Western blots were stained for phosphorylated (p)STAT3 and STAT3. Blots are representative of three independent experiments. Normalized band intensity data are means  $\pm$  SD from all experiments.  $*P \leq 0.05$ ,  $**P \leq 0.01$ ,  $***P \leq 0.001$  and  $****P \leq 0.0001$  by analysis of variance (ANOVA) test with Dunnett’s correction.

**Fig. 5: Potency-enhancing mutations minimize IL-11 trans-signaling inhibition by sgp130Fc.** **(A)** Schematic representation of sgp130<sup>T102Y/Q113F/N114L</sup>Fc with enhanced affinity for IL-6. **(B)** Ba/F3-gp130 cells were incubated with 50 ng/ml IL-6 and 100 ng/ml sIL-6R in the presence of increasing concentrations of sgp130Fc (closed rhombi) or the sgp130<sup>T102Y/Q113F/N114L</sup>Fc mutein (open rhombi) featuring a triple mutation that increases its affinity towards IL-6. **(C)** Ba/F3-gp130 cells were incubated with 10 ng/ml IL-11 and 100 ng/ml sIL-11R in the presence of increasing concentrations of sgp130Fc (closed rhombi) or sgp130<sup>T102Y/Q113F/N114L</sup>Fc (open rhombi). At 72 hours after stimulation, cellular proliferation was assessed using a CellTiter-Blue assay and normalized as described in the Methods. Data are representative of three independent experiments.

**Fig. 6: Affinity-enhancing mutations improve inhibitory capacity and selectivity of cs-130Fc variants.** (A and B) Ba/F3-gp130 cells were stimulated with 50 ng/ml IL-6 and 100 ng/ml sIL-6R (A) or 10 ng/ml IL-11 and 100 ng/ml sIL-11R (B) in the presence of increasing inhibitor concentrations. At 72 hours after stimulation, cellular proliferation was detected using a CellTiter-Blue assay and normalized as described in the Methods. Data are from three independent experiments.

**Fig. 7: cs-130Fc variants efficiently block T<sub>H</sub>17 cell expansion.** (A and B) Naïve CD4<sup>+</sup> T-cells (CD4<sup>+</sup>CD25<sup>-</sup>CD44<sup>lo</sup>CD62L<sup>hi</sup>) from *IL6ra*<sup>-/-</sup> mice were cultured in Iscove's Modified Dulbecco's Medium supplemented with TGFβ (1 ng/mL), IL-23 (20 ng/mL), IL-6 (50 ng/mL), sIL-6R (100 ng/mL), and anti-IL-2 (10 ng/mL) in the presence of increasing concentrations of the indicated inhibitor. To monitor T<sub>H</sub>17 cell expansion, IL-17 production was assessed by flow cytometry. Histograms (A) and dose-response-curves with non-linear regression analysis (B) were plotted as percent inhibition normalized to controls. Data are means ± SD from three replicates.

Inhibitor	Theoretical MW (kDa)	SEC-MALS MW (kDa)
sgp130Fc	240	240.4 (± 0.2%)
cs-130Fc	157	184.7 (± 0.2%)
cs-130	52	75.0 (± 1.1%)
c <sub>GFP8</sub> -130Fc	153	179.9 (± 0.2%)
cs-130 <sup>Y190K/F191E</sup> Fc	157	191.7 (± 0.6%)

**Table 1: SEC-MALS analysis of purified proteins.** The absolute weight-averaged molar mass ( $M_w$ ) of affinity purified sgp130Fc and cs-130Fc variants was analyzed by SEC-MALS. Between 10 and 50 μg were injected per sample on a Superpose 6 Increase column in PBS (pH 7.0) at a flow rate of 0.5 ml/min and analyzed using a Multi-Angle Light Scattering (MALS) system (Wyatt Technology).

Inhibitor	Stimulation cytokine (ng/ml)	IC <sub>50</sub>	
		ng/ml	nM
sgp130Fc	IL-6/sIL-6R (50/100)	226.1 ± 176.3	0.87 ± 0.68
sgp130 <sup>T102Y/Q113F/N114L</sup> Fc	sIL-6R/IL-6 (50/100)	70.1 ± 34.0	0.27 ± 0.18
cs-130Fc	sIL-6R/IL-6 (50/100)	86.4 ± 73.7	0.46 ± 0.39
cs-130	sIL-6R/IL-6 (50/100)	102.0 ± 102.1	1.46 ± 1.46
c <sub>GFP</sub> S-130Fc	sIL-6R/IL-6 (50/100)	1243.0 ± 957.6	6.54 ± 5.04
cs-130 <sup>Y190K/F191E</sup> Fc	sIL-6R/IL-6 (50/100)	1963.3 ± 1153.9	7.55 ± 6.07
cs-130 <sup>T102Y/Q113F/N114L</sup> Fc	sIL-6R/IL-6 (50/100)	68.2 ± 29.5	0.36 ± 0.16
cs-130 <sup>T102Y/Q113F/N114L</sup>	sIL-6R/IL-6 (50/100)	33.5 ± 14.9	0.48 ± 0.08
sgp130Fc	sIL-11R/IL-11 (10/100)	56.4 ± 5.8	0.22 ± 0.02
sgp130 <sup>T102Y/Q113F/N114L</sup> Fc	sIL-11R/IL-11 (10/100)	No inhibition	No inhibition
cs-130Fc	sIL-11R/IL-11 (10/100)	1355.9 ± 697.1	7.14 ± 3.77
cs-130	sIL-11R/IL-11 (10/100)	No inhibition	No inhibition
c <sub>GFP</sub> S-130Fc	sIL-11R/IL-11 (10/100)	3181.5 ± 2834.8	16.67 ± 14.92
cs-130 <sup>Y190K/F191E</sup> Fc	sIL-11R/IL-11 (10/100)	No inhibition	No inhibition
cs-130 <sup>T102Y/Q113F/N114L</sup> Fc	sIL-11R/IL-11 (10/100)	No inhibition	No inhibition
cs-130 <sup>T102Y/Q113F/N114L</sup>	sIL-11R/IL-11 (10/100)	No inhibition	No inhibition

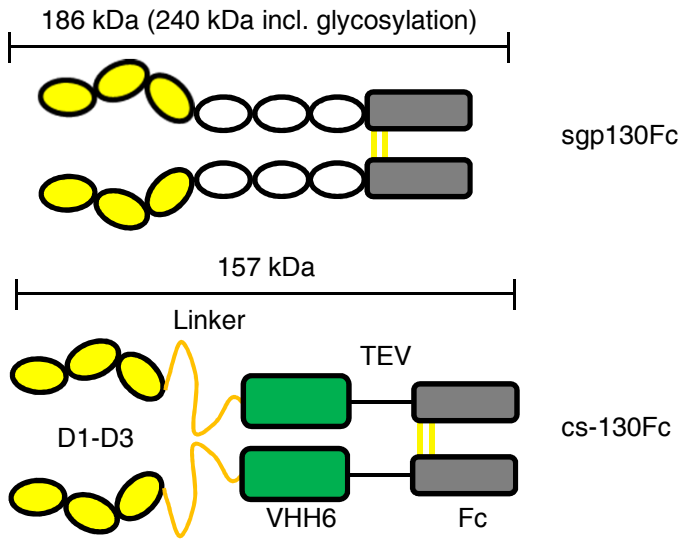
**Table 2: Inhibitory profile of sgp130 and chimeric soluble sgp130 fusion proteins.** Ba/F3-gp130 cells were stimulated with the indicated concentrations of cytokines and their respective soluble  $\alpha$ -receptors in the presence of decreasing inhibitor concentrations. IC<sub>50</sub> values were determined from three independent experiments.

	k <sub>on</sub> (1/M.s)	T(k <sub>on</sub> )	k <sub>off</sub> (1/s)	T(k <sub>off</sub> )	K <sub>d</sub> (M)
sgp130Fc	8.6E+5	1.1E+2	2.7E-6	2.4	3.1E-11
cs-130Fc	4.6E+4	4.3E+2	3.9E-4	7.7E-6	8.6E-9

**Table 3: Kinetic parameters of inhibitor interaction with hyper-IL-11-Fc.** Surface plasmon resonance analysis of hyper-IL-11-Fc binding to purified sgp130Fc and cs-130Fc. Hyper-IL-11-Fc was immobilized on a CM-5 chip and increasing concentrations of inhibitors (5–80 nM) were injected at a flow rate of 30  $\mu$ l/min. Measurements were carried out on a Biacore X100 instrument.

Figure 1

A



B

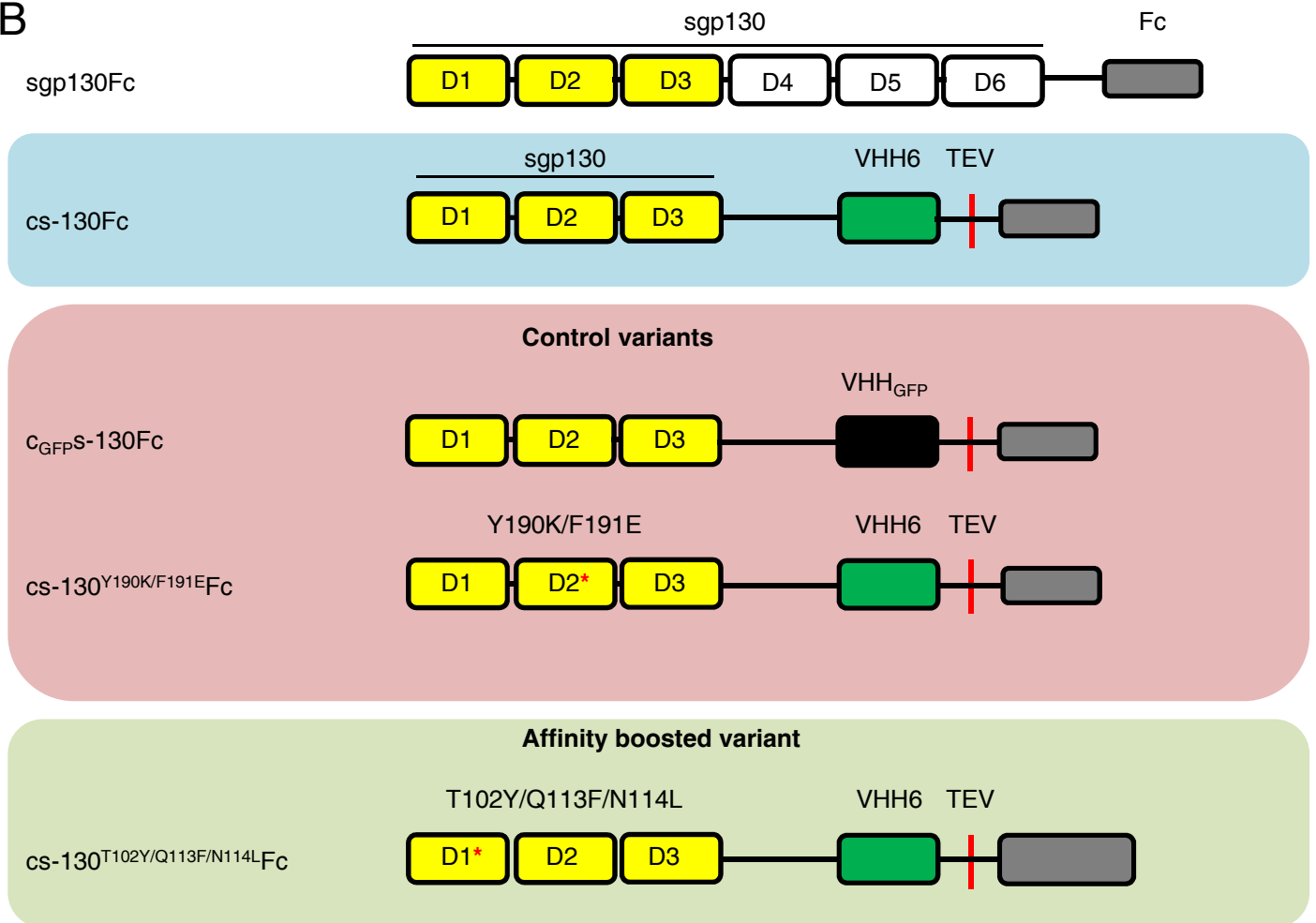
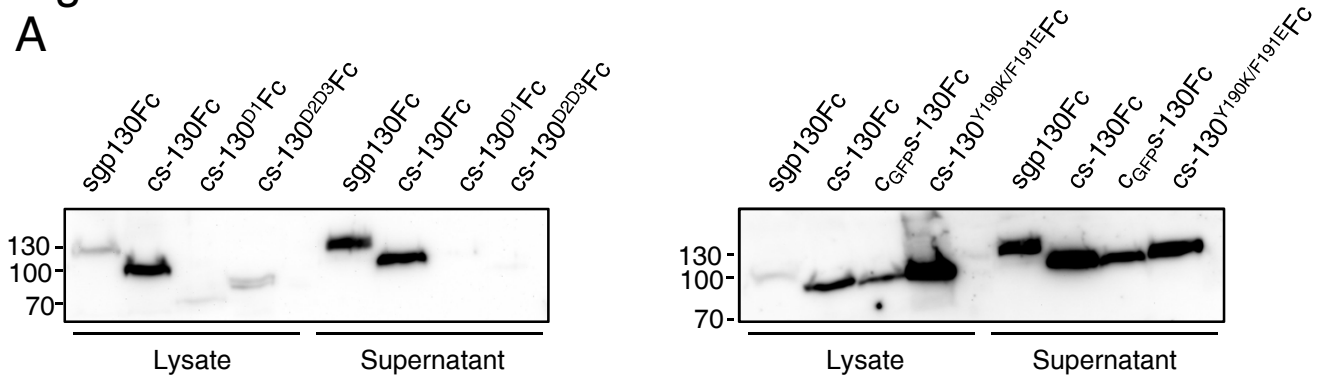
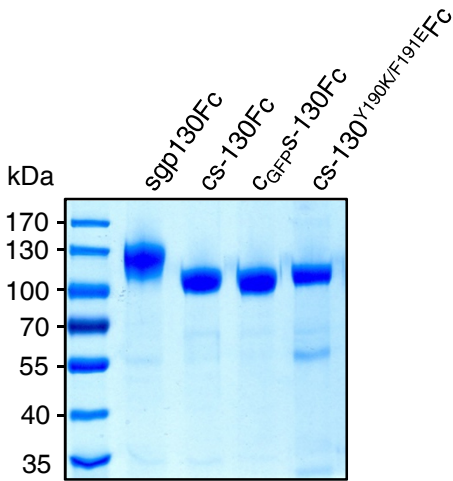


Figure 2

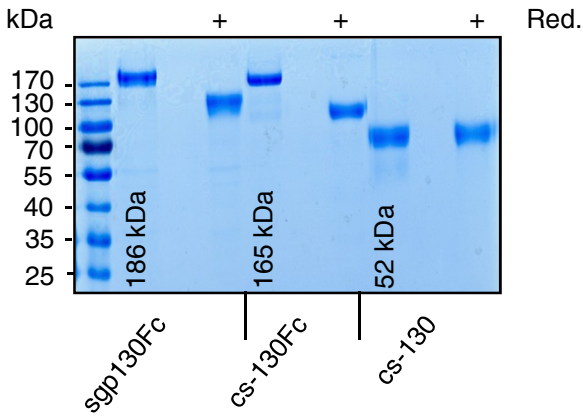
A



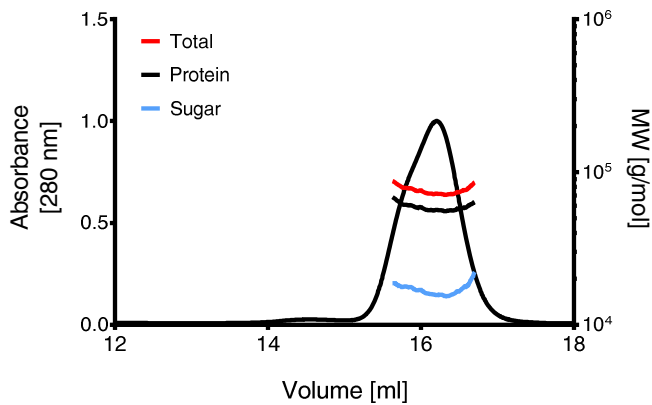
B



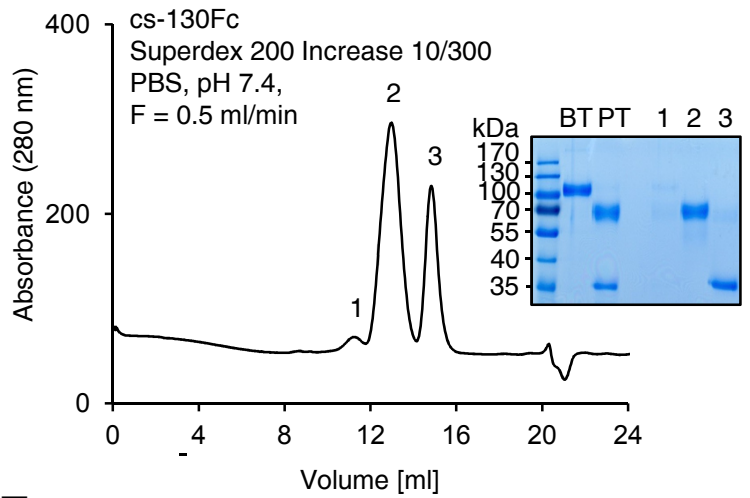
D



F



C



E

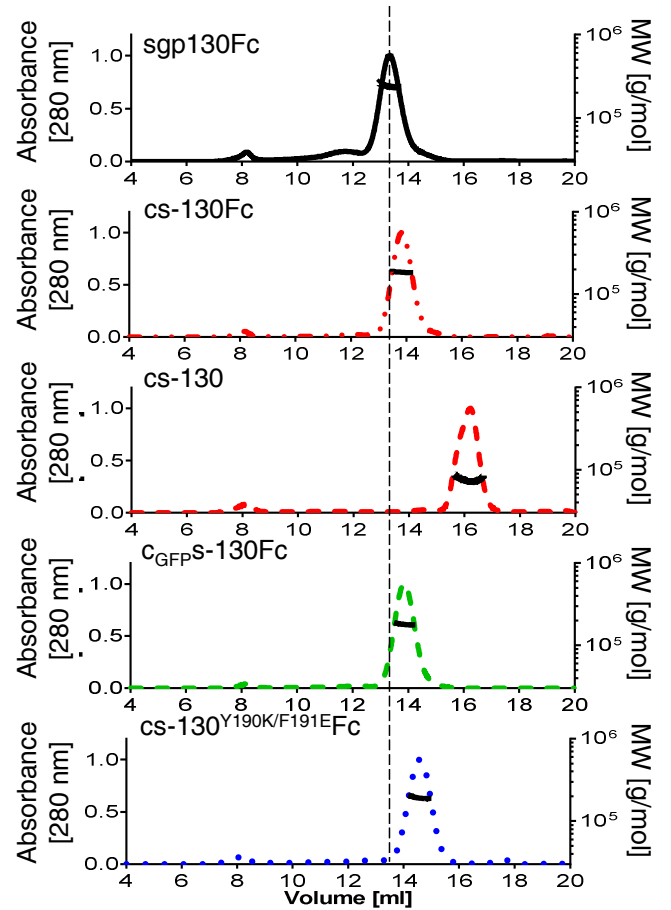
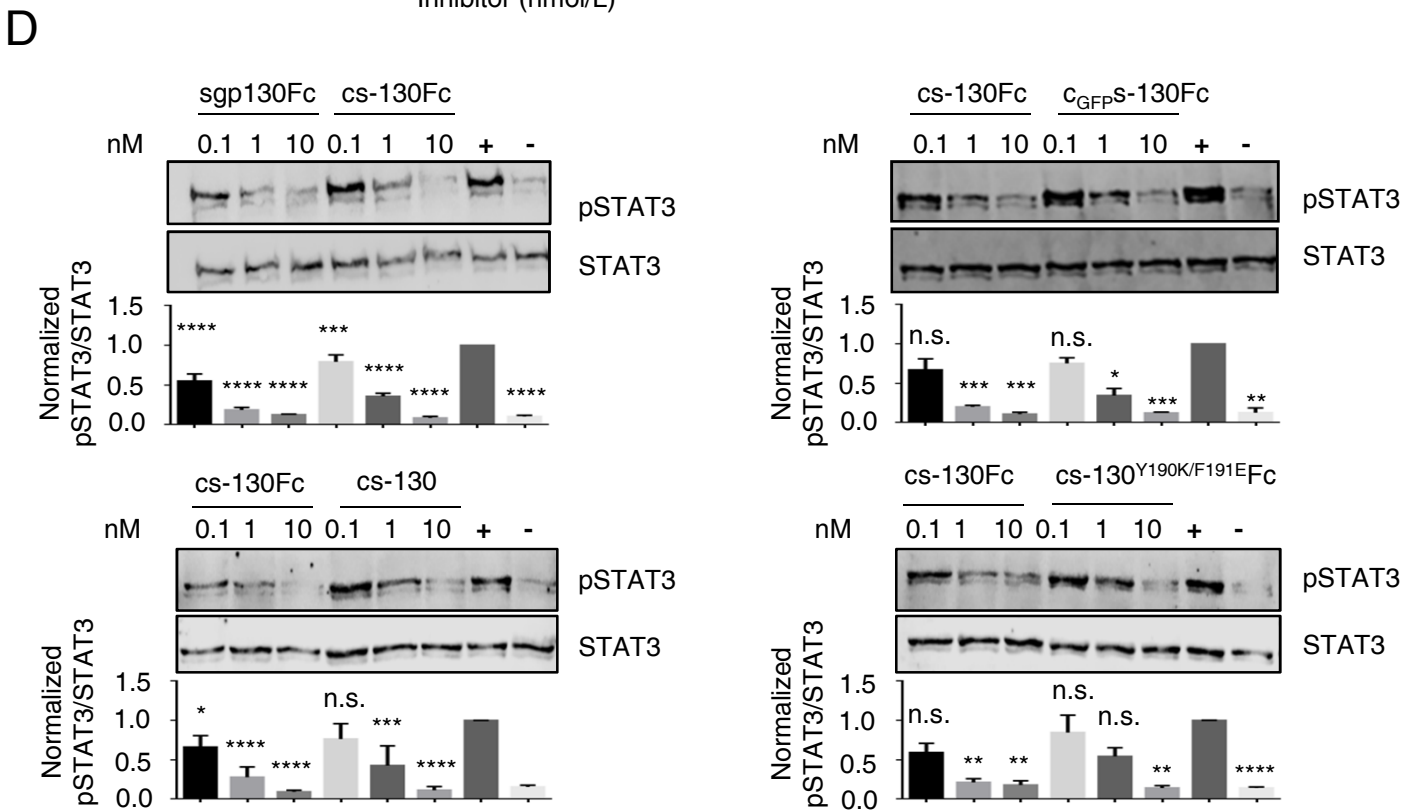
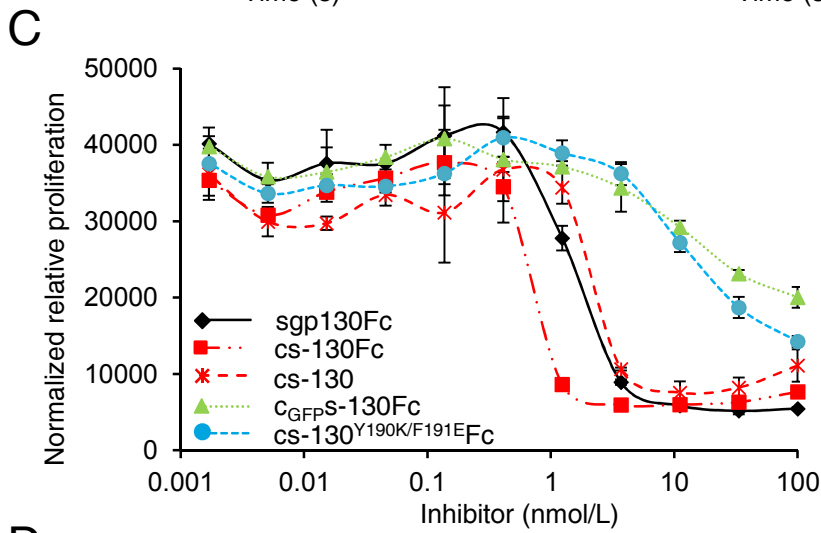
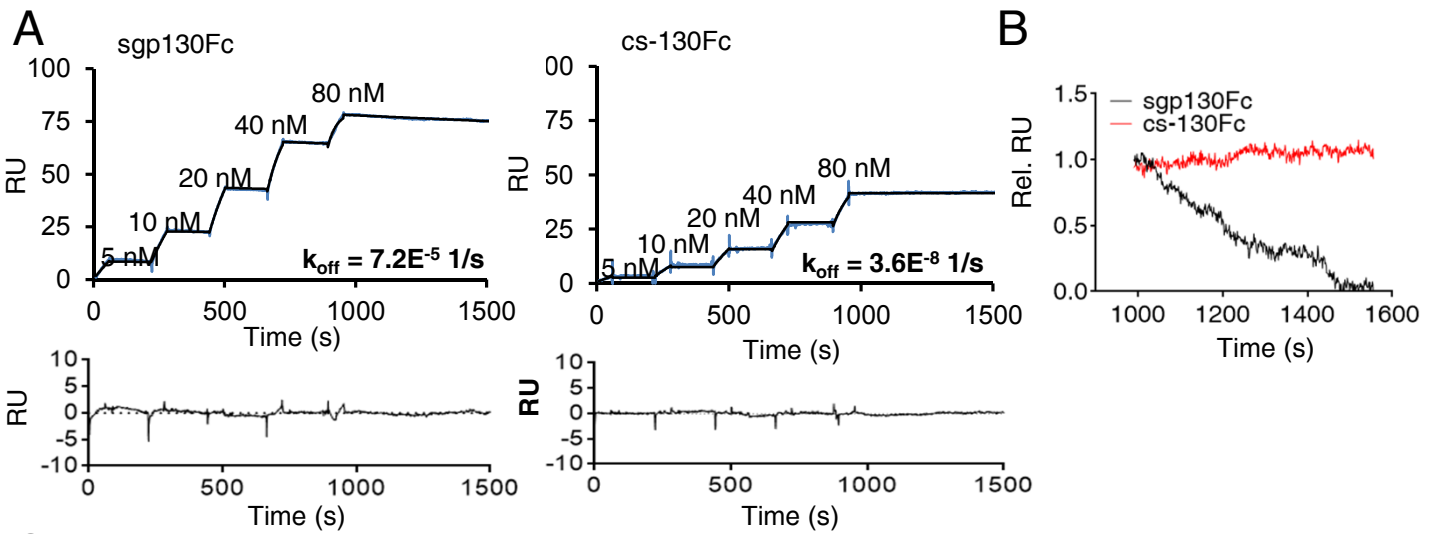


Figure 3



**Figure 4**

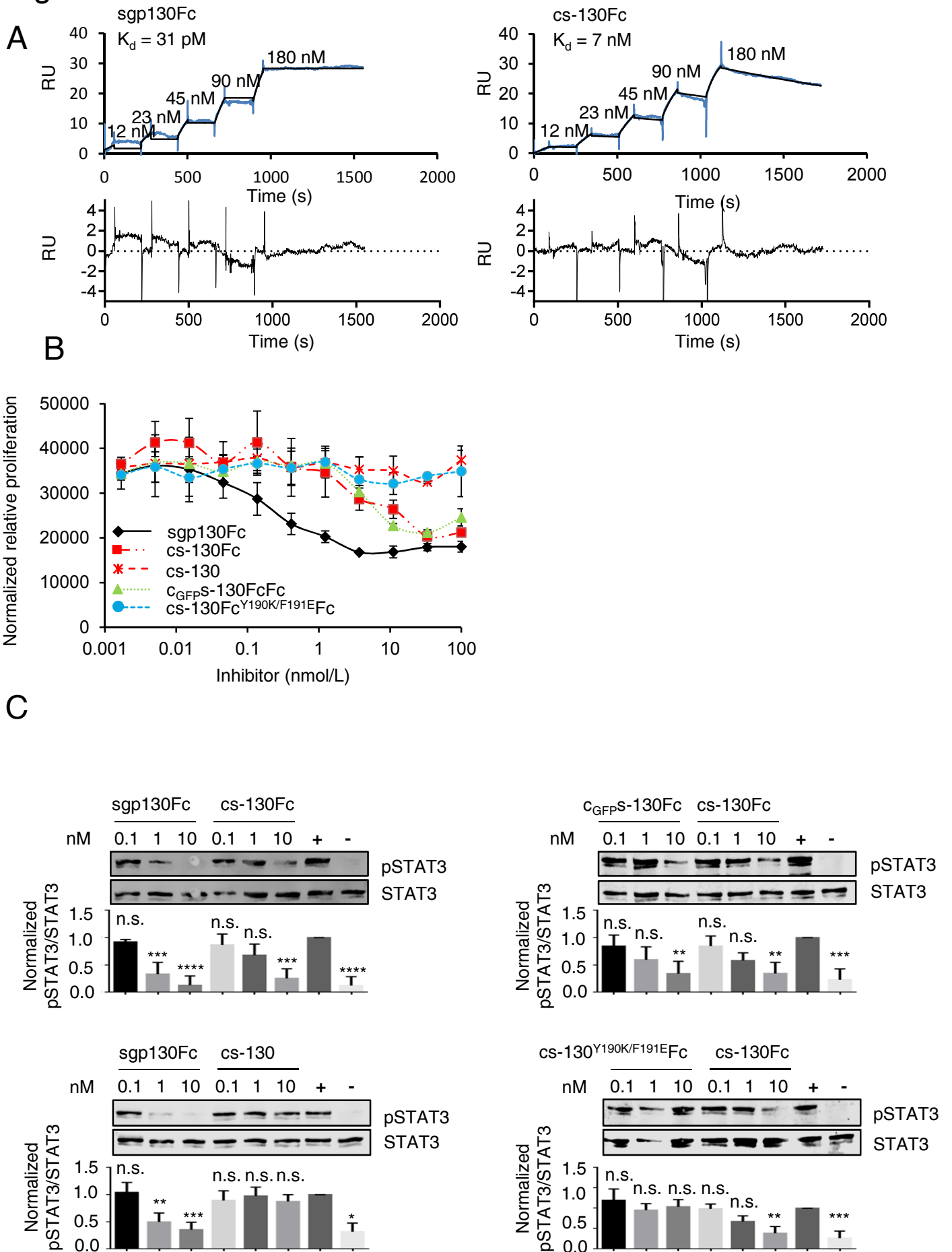
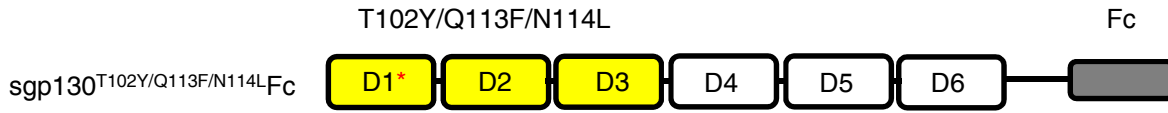
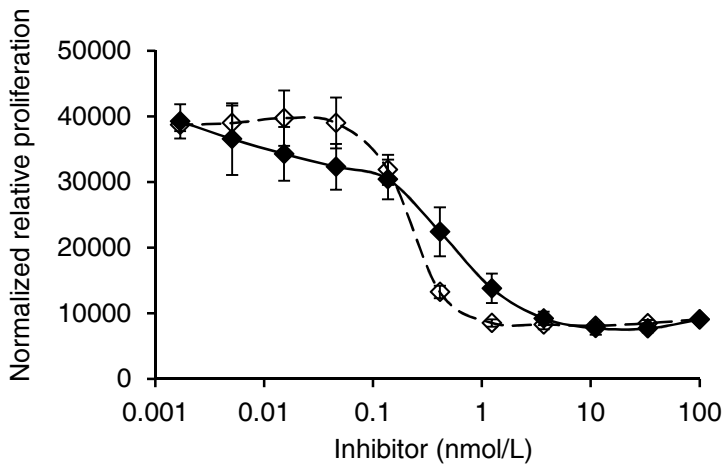


Figure 5

A



B



C

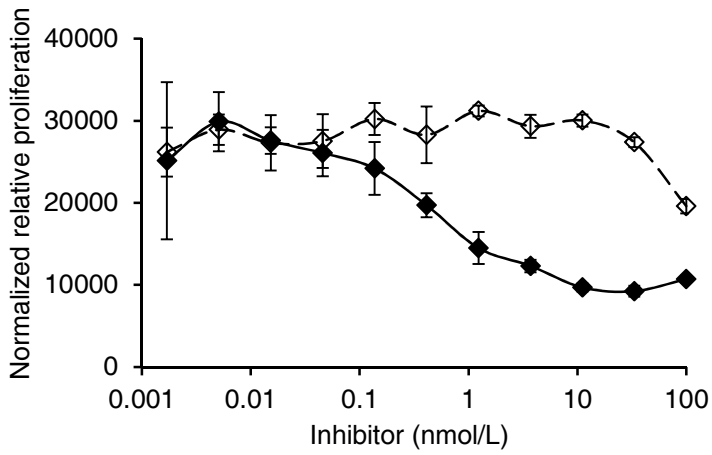
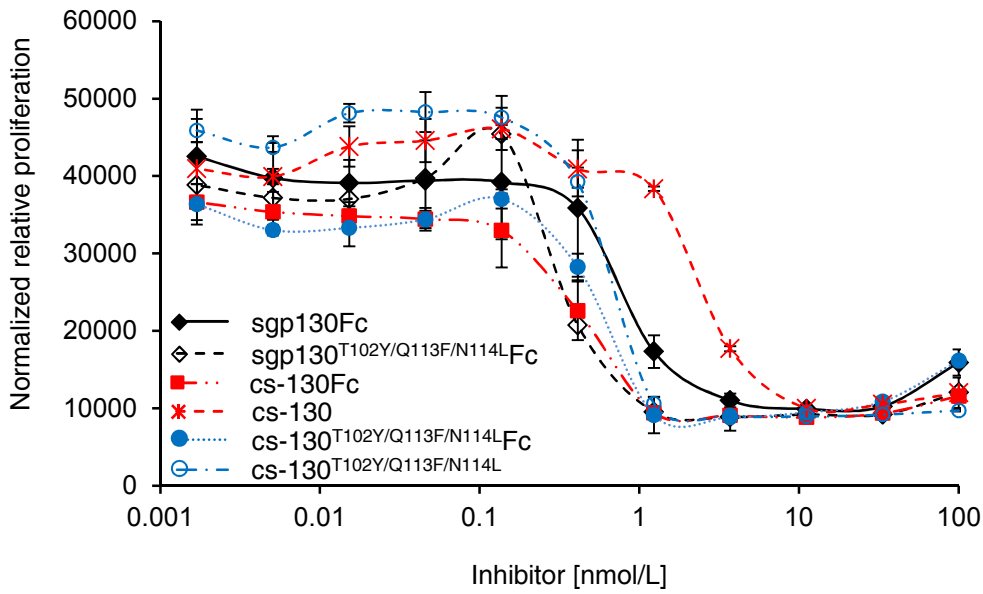


Figure 6

A



B

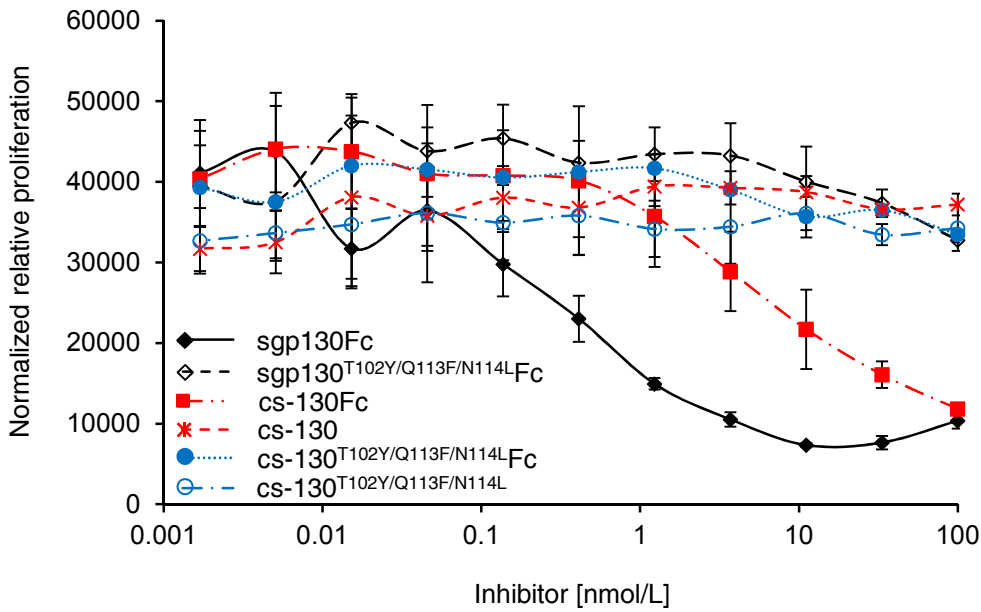
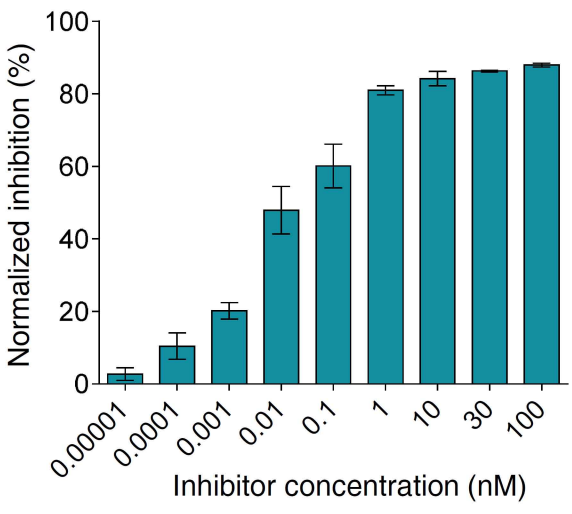
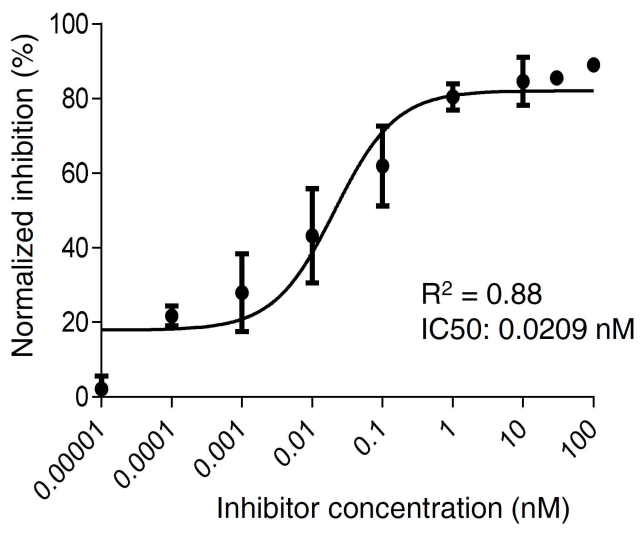
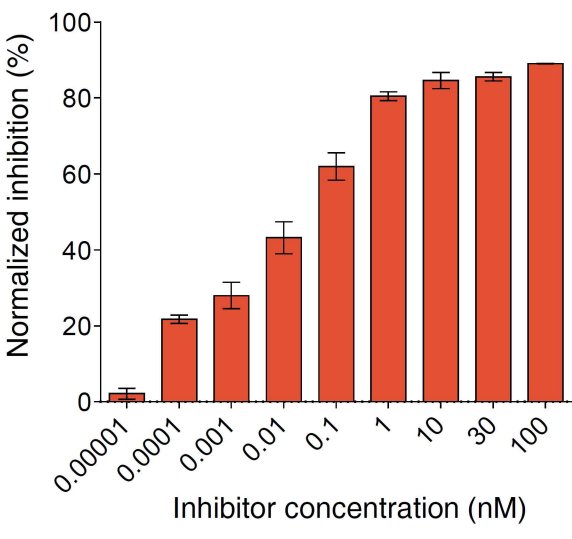
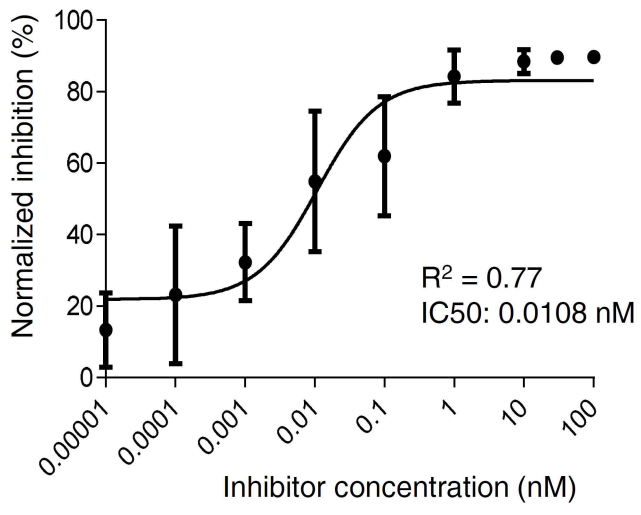
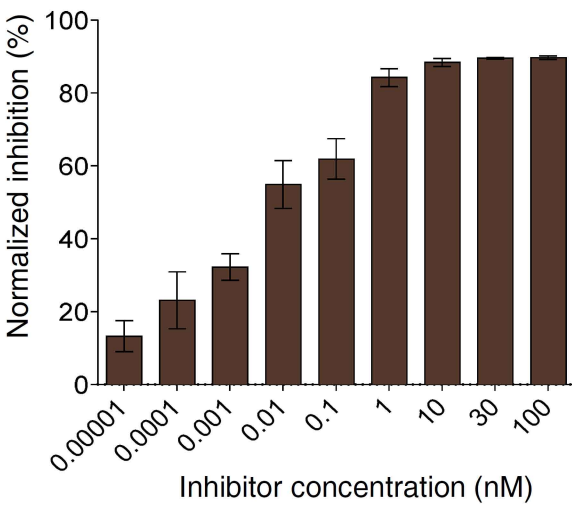
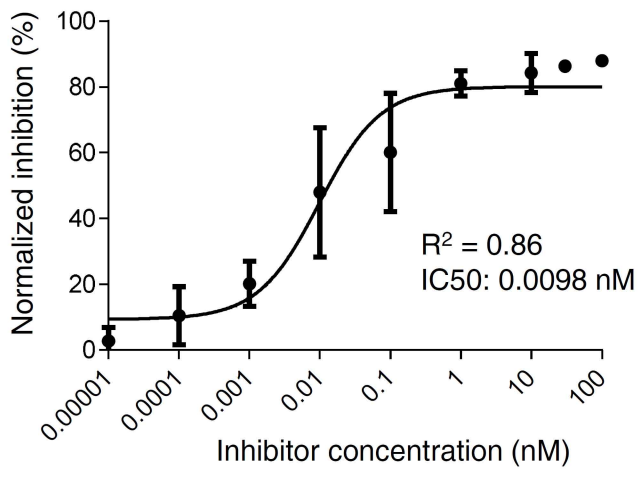


Figure 7

A



B



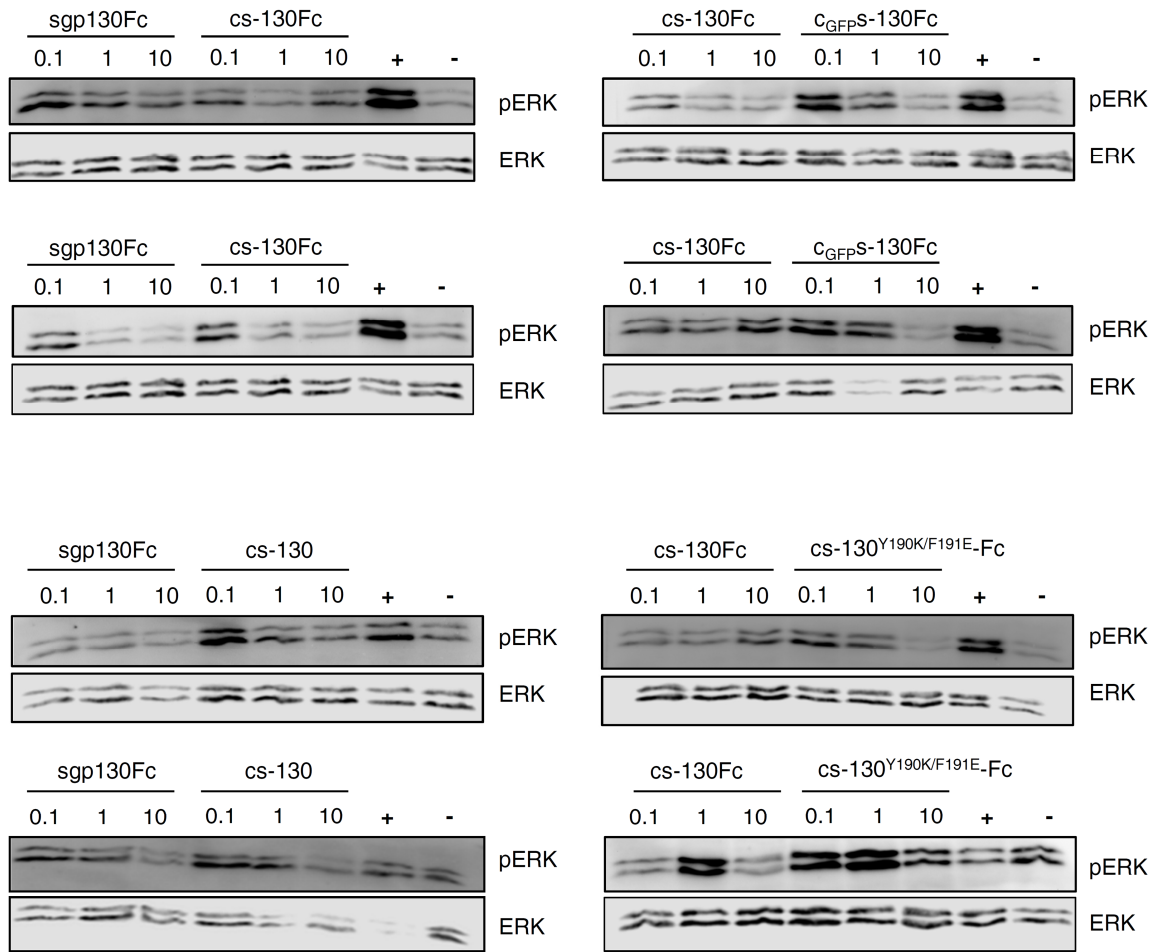


**Figure S1: cs-130 variants inhibit IL-6 trans-signaling induced ERK phosphorylation.** Western blot analysis of Ba/F3-gp130 cells stimulated for 30 min with 50 ng/ml IL-6 and 100 ng/ml sIL-6R (“+” lane) in the presence of the indicated concentrations of sgp130Fc, cs-130 or cs-130Fc variants. Prior to stimulation, IL-6, sIL-6R and inhibitors were incubated separately for 30 min. Western blots were stained for phosphorylated (p)ERK and ERK. Western blots are representative of N = 2 independent experiments. Both replicates are shown.

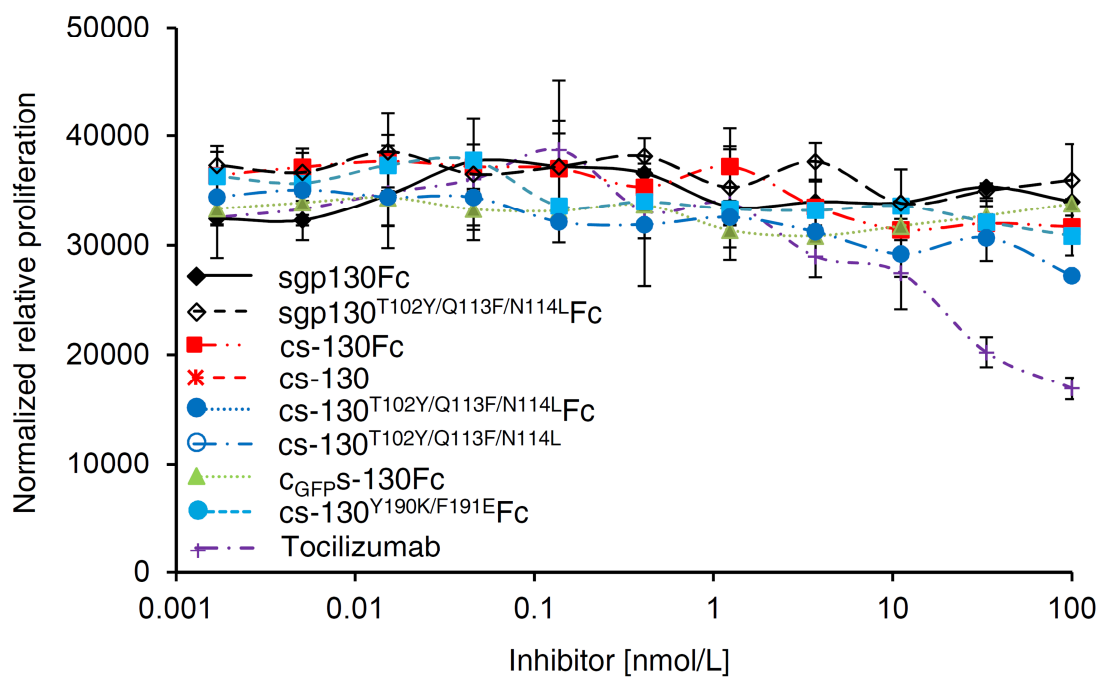


**Figure S2: cs-130(Fc) variants do not affect IL-6 classic signaling.** (A) Ba/F3-gp130-IL-6R cells were stimulated with 10 ng/ml IL-6 in the presence of increasing inhibitor concentrations. As a control for the inhibition of IL-6 classic-signaling, the clinically approved IL-6R-neutralizing antibody tocilizumab was used. At 72 hours after stimulation, cellular proliferation was detected using a CellTiter-Blue assay. Normalization of relative proliferation was performed as described in Methods. Assays are representative of three independent experiments.

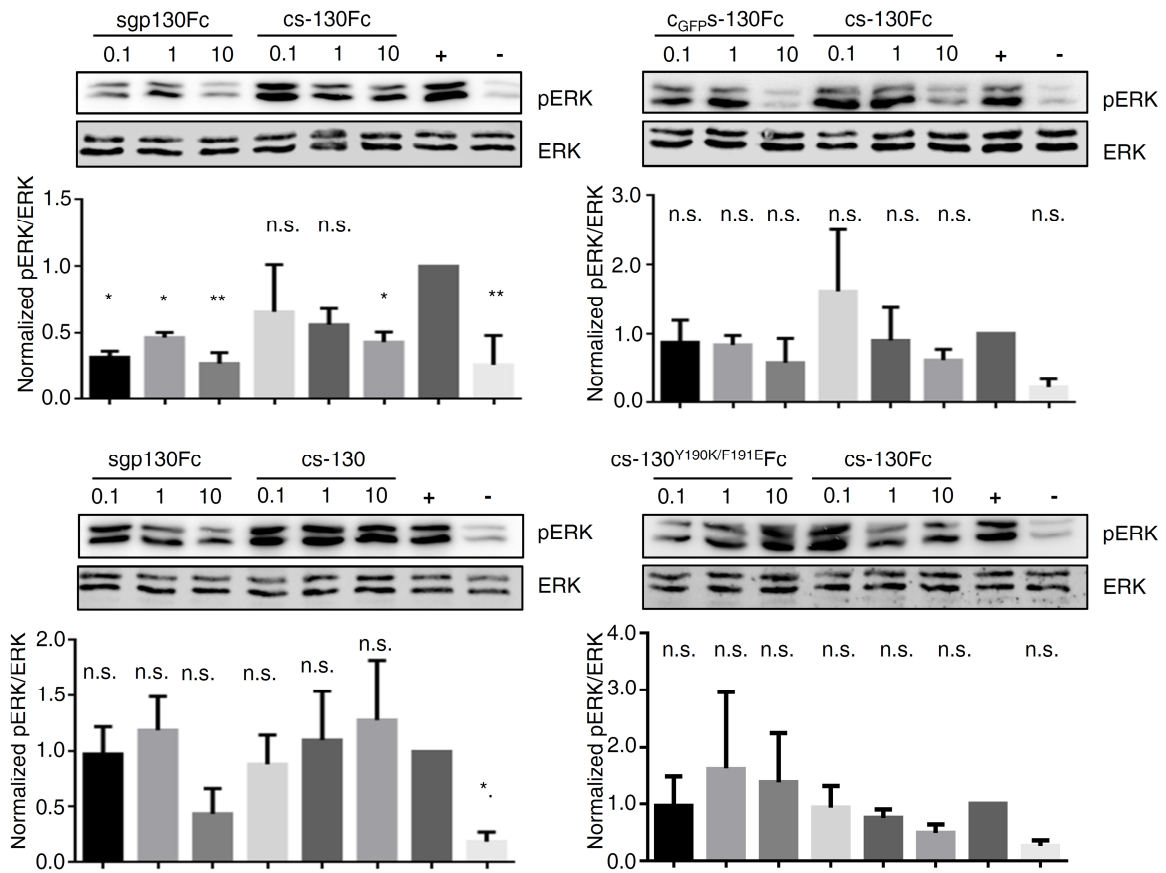


**Figure S3: cs-130Fc variants have reduced effect on IL-11 trans-signaling.** Western blot analysis of Ba/F3-gp130 cells stimulated for 30 min with 400 ng/ml IL-11 and 800 ng/ml sIL-11R (“+” lane) in the presence of the indicated inhibitor concentrations. Prior to stimulation, IL-11, sIL-11R and inhibitors were incubated separately for 30 min. Western blots were stained for phosphorylated (p)ERK and ERK. Western blots are representative of N = 3 independent experiments. Normalized band intensity data are means  $\pm$  SD from all experiments. \* $P \leq 0.05$ , \*\* $P \leq 0.01$ , \*\*\* $P \leq 0.001$  and \*\*\*\* $P \leq 0.0001$  (or n.s., not significant) by analysis of variance (ANOVA) test with Dunnett’s correction.

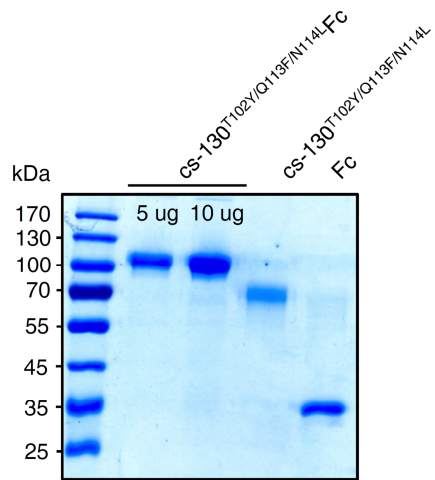


**Figure S4: cs-130<sup>T102Y/Q113F/N114L</sup>Fc is readily purified by affinity chromatography.** SDS-PAGE analysis of purified cs-130<sup>T102Y/Q113F/N114L</sup>Fc. After affinity purification of cs-130<sup>T102Y/Q113F/N114L</sup>Fc, the Fc fragment was removed by TEV protease-mediated proteolysis. The resulting fragments were separated by SEC and analyzed by SDS-PAGE and stained with Coomassie brilliant blue.

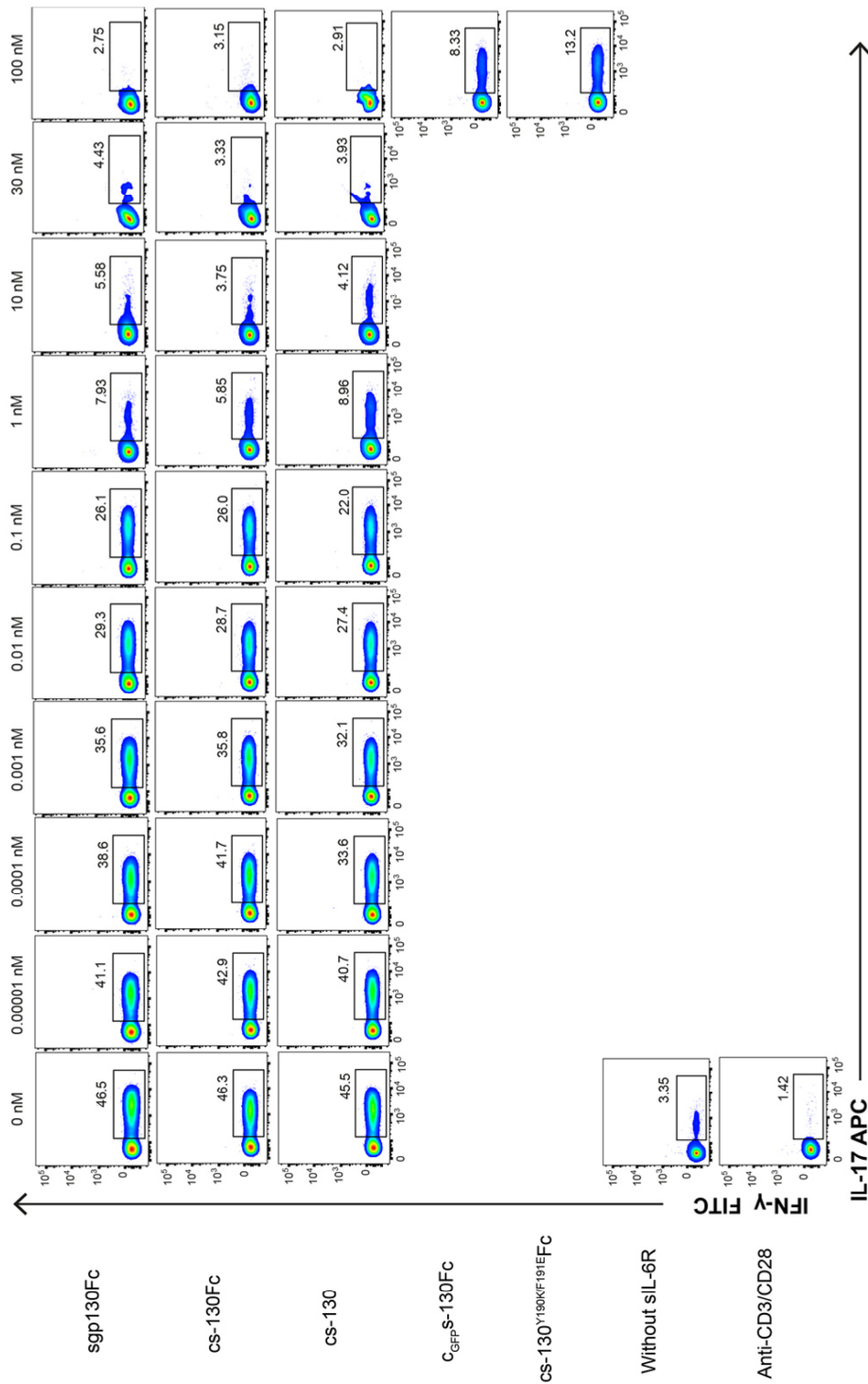


**Figure S5: Flow cytometric analysis of cs-130Fc variant mediated inhibition of T<sub>H</sub>17 cell expansion.** Representative flow cytometry plots (n= 3) of naïve CD4<sup>+</sup> T-cells (CD4<sup>+</sup>CD25<sup>-</sup>CD44<sup>lo</sup>CD62L<sup>hi</sup>) from *IL-6ra*<sup>-/-</sup> mice cultured in vitro under polarising conditions for T<sub>H</sub>17 cells [TGFβ (1 ng/mL), IL-23 (20 ng/mL), IL-6 (50 ng/mL), sIL-6R (100 ng/mL), and anti-IL-2 (10 ng/mL)] in the presence of increasing inhibitor concentrations, as indicated, for 4 days. T<sub>H</sub>17 cell differentiation was determined by flow cytometry after stimulation with PMA, ionomycin, and monensin for 4 hours.

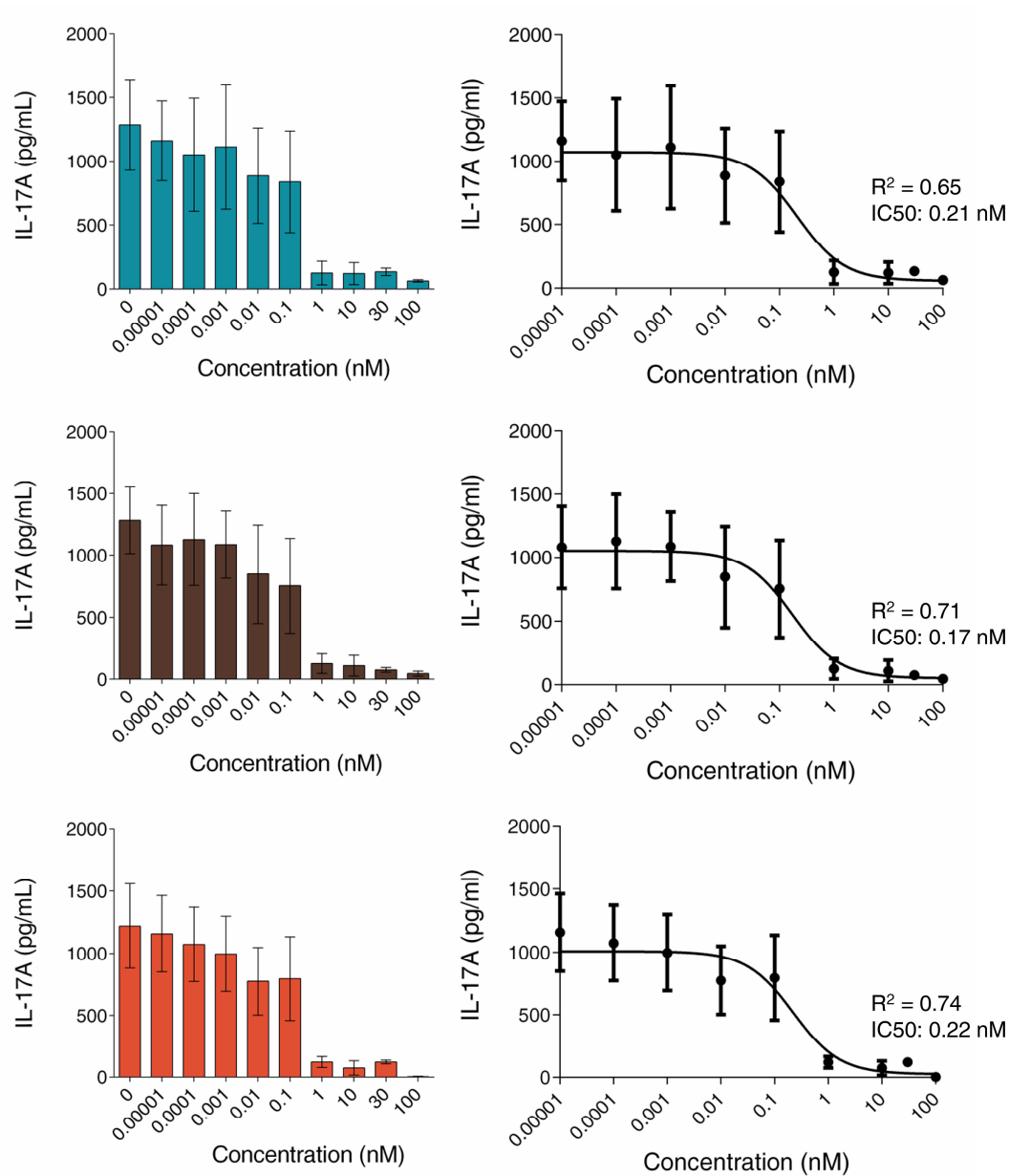


**Figure S6: cs-130 variants prevent IL-17 secretion from naïve T cells stimulated under polarizing conditions for  $T_H17$  expansion.** Naïve  $CD4^+$  T-cells ( $CD4^+CD25^-CD44^{lo}CD62L^{hi}$ ) were isolated from *IL6ra*<sup>-/-</sup> mice and cultured under  $T_H17$ -polarizing conditions [TGF $\beta$  (1 ng/mL), IL-23 (20 ng/mL), IL-6 (50 ng/mL), sIL-6R (100 ng/mL), and anti-IL-2 (10 ng/mL)] in the presence of increasing concentrations of sgp130Fc, cs-130Fc or cs-130 for 4 days. IL-17 secretion was determined by ELISA after stimulation with PMA, ionomycin and monensin for 4 hours (left), and non-linear regression analysis of the ELISA data was performed to determine  $IC_{50}$  values (right).